arXiv:2508.15220v1 [cs.LG] 21 Aug 2025

Locally Pareto-Optimal Interpretations for Black-Box Machine Learning Models*

Aniruddha Joshi[1], Supratik Chakraborty[2], S Akshay[2], Shetal Shah[2], Hazem Torfah[3], and Sanjit Seshia[1]

[1] University of California at Berkeley, USA
{aniruddhajoshi, sseshia}@berkeley.edu
[2] Indian Institute of Technology Bombay, India
{ supratik, akshayss, shetals}@cse.iitb.ac.in
[3] Chalmers University of Technology and University of Gothenburg. Sweden
hazemto@chalmers.se

Abstract. Creating meaningful interpretations for black-box machine learning models involves balancing two often conflicting objectives: accuracy and explainability. Exploring the trade-off between these objectives is essential for developing trustworthy interpretations. While many techniques for multi-objective interpretation synthesis have been developed, they typically lack formal guarantees on the Pareto-optimality of the results. Methods that do provide such guarantees, on the other hand, often face severe scalability limitations when exploring the Pareto-optimal space. To address this, we develop a framework based on local optimality guarantees that enables more scalable synthesis of interpretations. Specifically, we consider the problem of synthesizing a set of Pareto-optimal interpretations with local optimality guarantees, within the immediate neighborhood of each solution. Our approach begins with a multi-objective learning or search technique, such as Multi-Objective Monte Carlo Tree Search, to generate a best-effort set of Pareto-optimal candidates with respect to accuracy and explainability. We then verify local optimality for each candidate as a Boolean satisfiability problem, which we solve using a SAT solver. We demonstrate the efficacy of our approach on a set of benchmarks, comparing it against previous methods for exploring the Pareto-optimal front of interpretations. In particular, we show that our approach yields interpretations that closely match those synthesized by methods offering global guarantees.

* The work of S. Chakraborty was partly supported by a Qualcomm Faculty Award. The work of S. Akshay was partly supported by the SBI Foundation Hub for Data Science & Analytics, IIT Bombay. The UC Berkeley authors were partly supported by the DARPA Provably Correct Design of Adaptive Hybrid Neuro-Symbolic Cyber Physical Systems (ANSR) program award number FA8750-23-C-0080, and by Nissan and Toyota under the iCyPhy Center. The work of H. Torfah was partly supported by the Wallenberg AI, and Autonomous Systems and Software Program (WASP) funded by the Knut and Alice Wallenberg Foundation.
This work has been accepted at ATVA 2025.

1 Introduction

The use of machine learning (ML) components is rapidly increasing across various applications and domains. However, the complexity of ML models often makes it difficult to understand how these components function. As a result, their behavior is frequently treated as a black box. To build trust in ML models, especially in domains where accountability and safety are critical, it is essential to provide interpretations that accurately reflect the underlying functionality of the ML model, while being also understandable by humans.

Over the past decade, a vast body of research has focused on explaining the behavior of ML models (e.g, see [16] for a survey). A prominent approach in this area has been the development of post-hoc interpretation methods, i.e., techniques used to explain the behavior of an ML model after it has been trained. These methods often involve generating surrogate models (e.g., decision trees, decision lists, etc.) that serve as simplified approximations of the original complex model [16]. A key challenge in creating such models lies in finding the right balance between accuracy and explainability. In many cases, these two objectives are in direct conflict: a simple, human-understandable explanation may diverge significantly from the predictions of the original model, while a more accurate surrogate may be too complex for meaningful human interpretation. This raises a central question: how much accuracy are users willing to sacrifice for the sake of explainability, and vice versa?

While there are no easy answers to the above problem, a promising way to address it is by exploring the Pareto-optimal space of interpretations [35]. Rather than generating a single interpretation optimized for one objective (or even for a weighted combination of objectives), the Pareto-optimal interpretation problem involves examining the trade-off across multiple objectives, such as the balance between accuracy and explainability. This approach can be very beneficial for users aiming to understand these trade-offs; however, it also introduces significant challenges, particularly in efficiently navigating the space of possible interpretations. Previous work has demonstrated that it is possible to explore this space with formal statistical guarantees on the explored Pareto-optimal curve [35]. However, these approaches often struggle to scale due to their full reliance on computationally intensive symbolic techniques like constraint solvers. In this paper, we address the question of whether lighter and faster methods can be used to generate candidate Pareto-optimal interpretations, which can then be refined using more powerful tools such as Boolean satisfiability solvers.

Specifically, we propose the use of Multi-Objective Monte Carlo Tree Search (MO-MCTS) [36], a well-established technique from the field of reinforcement learning known for its strong empirical performance, to quickly approximate the Pareto-optimal curve. We integrate MO-MCTS with Boolean satisfiability solving, enabling us to obtain local guarantees on the Pareto-optimality of interpretations. This replaces earlier global Pareto-optimality guarantees with theoretically weaker local Pareto-optimality. However, since MO-MCTS is capable of recovering global guarantees over time, running our approach for a sufficient number of iterations yields interpretations whose local guarantees converge toward global

ones. In our experiments, we show empirical evidence that the local guarantees obtained using MO-MCTS within a reasonable timeout are indeed close to the global guarantees. The notion of locally Pareto-optimal interpretations, that we introduce, also offers additional benefits. Theoretically, they support anytime guarantees, meaning that useful solutions can be extracted at any point during execution (unlike earlier MaxSAT-based approaches). Additionally, they capture locally imperturbable interpretations, where small changes in the interpretation do not alter the optimality within a local neighborhood.

In summary our contributions are the following:

1. We formalize the problem of locally Pareto-optimal interpretation synthesis for black-box ML models, where explainability is traded off for accuracy under user control.
2. We develop a new technique to solve the above problem by a two phase hybrid algorithm that integrates Multi-objective Monte-Carlo Tree search with Boolean satisfiability solving.
3. We show that our approach converges monotonically to the global optimal, with local optimality guarantees for early stopping.
4. Our experimental results show that in practice, our approach obtains results close to the global optimal in several benchmarks. For larger benchmarks, we obtain results (with local optimality guarantees), where earlier approaches fail to produce *any* globally Pareto-optimal solution.

Related Work The literature contains a significant body of work focused on methods for interpreting black-box ML models. In certain applications, the goal is to explain the output of a black-box model in the vicinity of a specific input. To achieve this, specialized techniques have been developed that provide local and robust explanations [15,22,28,29]. Other applications use techniques like generation of surrogate models and model distillation (in the form of decision trees [19,12,18,20,37]). For further information on these techniques, we refer the reader to the surveys in [4,16].

The problem of synthesizing multi-objective interpretations of black-box ML models was introduced and formalized in [35]. In that work, a MaxSAT-based engine was used to synthesize a set of Pareto-optimal interpretations. This approach provides statistical global guarantees on the accuracy of the synthesized interpretations. Similar ideas were explored in [37], where the authors encoded the problem of finding an interpretation as optimal decision sets, and in [38], where sparse optimal decision trees were constructed using an objective function combining misclassification rate and the number of leaves. In comparison to the approach in [35], the solutions presented in [37] and [38] provide a single point in the Pareto-optimal space, yielding a single value for correctness and explainability measures. Our approach aligns with the goals of [35] in providing Pareto-optimal interpretations with guarantees on correctness. However, in contrast to [35], our method offers a much more scalable solution for exploring the Pareto-optimal front. In [10], the authors use multi objective optimization to find locally optimal Pareto solutions to the joint problem of generating a

machine learning model and its surrogate. Our work is agnostic to the machine learning model, which is assumed to be a black box.

Monte-Carlo Tree Search (MCTS) is a highly effective procedure for heuristically searching through a complex space of actions and rewards. Browne et al. [9] provide an excellent review on MCTS techniques and heuristics, and Swiechowski et al. [33] give a review of recent modifications and advances on domain specific adaptations required for MCTS. Other papers [36,11] consider the multi-objective variant of MCTS that is relevant to our work.

2 Preliminaries and Problem Formulation

We borrow some terminology from [35] in presenting the problem formulation below. Let $\mathcal{I}$ be an input domain, $\mathcal{O}$ be an output domain, and $\Delta(\mathcal{I} \times \mathcal{O})$ be a distribution over the input-output space induced by a black-box ML model. Let $\mathcal{G}$ denote the class of interpretations mapping $\mathcal{I}$ to $\mathcal{O}$. For each interpretation $g \in \mathcal{G}$, we abuse notation and define the semantic function $g : \mathcal{I} \to \mathcal{O}$ that outputs $g(i) \in \mathcal{O}$ for every input $i \in \mathcal{I}$. We also assume that each interpretation $g \in \mathcal{G}$ is associated with a non-negative real-valued *correctness measure* $\mathcal{C}(g) \in \mathbb{R}_{\geq 0}$, and a non-negative real-valued *explainability measure* $\mathcal{E}(g) \in \mathbb{R}_{\geq 0}$. Intuitively, $\mathcal{C}(g)$ measures the accuracy of the interpretation g w.r.t. the input-output distribution $\Delta(\mathcal{I} \times \mathcal{O})$, and $\mathcal{E}(g)$ is a user-specified measure of the human understandability of the interpretation. In general we want to synthesize interpretations with high values of correctness and explainability measures.

For an interpretation $g \in \mathcal{G}$, we define $(\mathcal{C}(g), \mathcal{E}(g))$ to be the *goodness tuple* of g. The partial order $\preceq$ on goodness tuples is defined as follows: $(c, e) \preceq (c', e')$ iff $c \leq c'$ and $e \leq e'$. The strict partial-order $\prec$ on such tuples is defined as: $(c, e) \prec (c', e')$ iff $(c, e) \preceq (c', e')$ and at least one of $c < c'$ or $e < e'$ holds. Given a set $\mathcal{S}$ of goodness measures (c, e), we define $\max^{\preceq}\ \mathcal{S}$ to be the set of all $\preceq$-maximal tuples in $\mathcal{S}$.

Definition 1 (Pareto-Domination and Optimality [21,35]). *Given a class $\mathcal{G}$ of interpretations mapping $\mathcal{I}$ to $\mathcal{O}$, we say an interpretation g Pareto-dominates another interpretation g' if $(\mathcal{C}(g'), \mathcal{E}(g')) \prec (\mathcal{C}(g), \mathcal{E}(g))$. An interpretation g is said to be **Pareto-optimal** (or PO) in $\mathcal{G}$ if $g \in \mathcal{G}$, and there is no other interpretation $g' \in \mathcal{G}$ that Pareto-dominates g. In other words, $(\mathcal{C}(g), \mathcal{E}(g))$ is $\preceq$-maximal in the set of goodness tuples of all interpretations in $\mathcal{G}$.*

In general, there may be multiple PO interpretations in $\mathcal{G}$, with one or more interpretations corresponding to each $\preceq$-maximal tuple (c, e). In [35], Torfah et al presented a technique to synthesize a set of PO interpretations, one for every $\preceq$-maximal tuple (c, e). This effectively gives the user a set of interpretations, none of which can be "improved" on both the accuracy and explainability measures together. Unfortunately, computing such PO interpretations is computationally expensive, and the technique of [35] does not scale large to problem instances. This motivates us to define locally Pareto-optimal interpretations.

Definition 2 (Locally Pareto-optimal interpretation). *Let $\mathcal{G}$ be a class of interpretations mapping $\mathcal{I}$ to $\mathcal{O}$, with correctness measure $\mathcal{C}(\cdot)$ and explainability measure $\mathcal{E}(\cdot)$, as before. Let $\delta_c \in \mathbb{R}_{\geq 0}$ be the* correctness slack*, and $\delta_e \in \mathbb{R}_{\geq 0}$ be the* explainabiility slack*, where $\mathbb{R}_{\geq 0}$ denotes the set of all non-negative reals. We say that an interpretation $g \in \mathcal{G}$ is locally Pareto-optimal (LPO) w.r.t δ_c and δ_e if $\nexists g' \in \mathcal{G}$ such that $(\mathcal{C}(g), \mathcal{E}(g)) \prec (\mathcal{C}(g'), \mathcal{E}(g')) \preceq (\mathcal{C}(g) + \delta_c, \mathcal{E}(g) + \delta_e)$.*

Informally, if interpretation g is LPO w.r.t. δ_c and δ_e, then there is no other interpretation g' that Pareto-dominates g, while having its correctness (respectively, explainability) measure within a window of δ_c (respectively, δ_e) of the corresponding measure for g. Note that an LPO interpretation g may not be a PO interpretation. However, there cannot be a "nearby" (in the correctness-explainability measure space) interpretation g' that improves the correctness (respectively, explainability) measure of g by an amount bounded by δ_c (respectively, δ_e) without adversely affecting explainability (respectively, correctness). Clearly, every PO intepretation is also LPO w.r.t δ_c and δ_e, for every $\delta_c, \delta_e \in \mathbb{R}_{\geq 0}$. We can now define the problem of synthesizing LPO interpretations as follows.

Problem 1 (Locally Pareto-Optimal Interpretation Synthesis). Let $\mathcal{G}$, $\mathcal{C}(\cdot)$, $\mathcal{E}(\cdot), \delta_c$ and δ_e be as in Definition 2. The *locally Pareto-optimal (or LPO)* interpretation synthesis problem requires us to synthesize a set $\mathcal{S}$ of interpretations in $\mathcal{G}$ s.t. every $g \in \mathcal{S}$ is LPO w.r.t δ_c and δ_e, and every distinct $g, g' \in \mathcal{S}$ are incomparable, i.e. neither of them Pareto-dominates the other.

A few points about Problem 1 are worth noting. First, the requirement that interpretations in the solution must not Pareto-dominate each other ensures that we don't report LPO interpretations, one of which dominates the other. This can indeed happen for LPO interpretations g and g' if, for example, $\mathcal{C}(g) > \mathcal{C}(g') + \delta_c$ and $\mathcal{E}(g) > \mathcal{E}(g') + \delta_e$. In such cases, g is a "better" interpretation than g', and it is not meaningful to report both g and g'. Second, every set of PO interpretations serves as a solution to Problem 1, for every non-negative value of δ_c and δ_e. However, not every LPO interpretation may be a PO interpretation in general. Hence, the ask of Problem 1 is weaker than that of finding PO interpretations (as addressed in [35]). Third, if we set δ_c and δ_e to M and N respectively, where $M > \max_{g \in \mathcal{G}} \mathcal{C}(g)$ and $N > \max_{g \in \mathcal{G}} \mathcal{E}(g)$, then every solution to Problem 1 also gives a set of PO interpretations. Hence, Problem 1 can be technically used to obtain PO interpretations, if we know $\max_{g \in \mathcal{G}} \mathcal{C}(g)$ and $\max_{g \in \mathcal{G}} \mathcal{E}(g)$. Finally, note that Problem 1 does not require us to synthesize a maximal (by subset ordering) set of incomparable LPO interpretations. This makes it possible to synthesize increasingly larger (set cardinality-wise) solutions incrementally.

3 Our Approach and the Problem Instantiation

In order to solve Problem 1, at a high level, we use a hybrid approach that has two phases. In the first phase, we use techniques developed from the multi-objective learning/search literature. We assume a time budget for the first phase,

and restrict ourselves to those techniques that maintain a best-effort solution at all times. Once the time budget is exhausted, we stop the first phase, retrieve the best-effort interpretations from the first phase, and then pass these interpretations to the second phase. We assume no guarantees about finding (locally) Pareto-optimal solutions from the first phase, since most multi-objective learning/search based techniques do not give strong anytime theoretical guarantees.

In the second phase, we take as inputs the set of interpretations obtained from the first phase, and also the correctness and explainability slacks δ_c and δ_e. We then verify that the interpretations obtained from the first phase are incomparable and also locally Pareto-optimal w.r.t. the given slacks. We do this in two steps. In the first step, we verify that the interpretations are incomparable. If they are not, we discard dominated interpretations. Then in the second step, we verify that the remaining interpretations are locally Pareto-optimal. If any of the interpretations are not locally Pareto-optimal, then we improve upon those interpretations. Thus, at the end we are able to output those interpretations that are incomparable and also locally Pareto-optimal. Figure 1 diagrammatically shows the two phases in our approach.

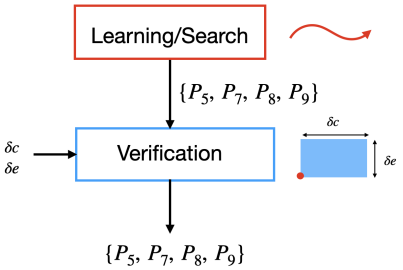

(a) The red curvy arrow represents a multi-objective search procedure with a time budget. If this outputs interpretations $\{P_5, P_7, P_8, P_9\}$, we then verify absence of a dominating solution within slack δ_c and δ_e, as represented by the blue rectangle.

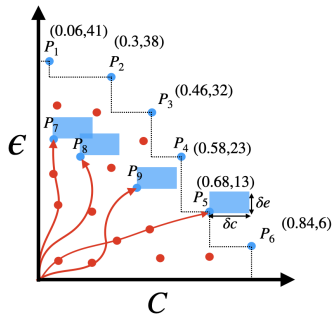

(b) Illustrating our navigation of the search space. The x-axis (resp. y-axis) represents the correctness (resp. explainability) measure. The red curvy arrows indicate the search based phase, and the blue rectangles indicate the verification phase. $P_1, \ldots P_6$ are PO interpretations. Our approach finds the LPO interpretations P_5, P_7, P_8, P_9

Fig. 1: Our approach

3.1 Instantiating the Interpretations and Measures

In order to solve Problem 1, we must first choose the class $\mathcal{G}$ of interpretations, and the explainability and correctness measures $\mathcal{C}(\cdot)$ and $\mathcal{E}(\cdot)$. We start by

choosing decision trees as the class of interpretations, since these are the most widely used in the explainable AI literature. Note that the work of [35] considers decision diagrams for interpretations. Decision trees are essentially decision diagrams with the additional restriction that every node has at most one incoming edge. Hence, we can use the same correctness and explainability measures as used in [35] , making it easier to compare our results with those of [35].

Class of Interpretations: Decision Trees Let $\mathcal{I}$ and $\mathcal{O}$ denote the input and output domains, respectively. We restrict the output domain $\mathcal{O}$ to a finite set $L := \{l_1, l_2, \ldots l_{|L|}\}$ of labels. Let $F := \{f_1, f_2, \ldots, f_{|F|} \mid f_i : \mathcal{I} \rightarrow \{1, 2, \ldots b_i\}\}$ be a set of functions f_i that map the input domain $\mathcal{I}$ to a finite set of branches $\{1, 2, \ldots b_i\}$. We use L and F to label the nodes of decision trees. Specifically, each internal node of a tree has an incoming edge and outgoing edges, and is labeled by a function f_i. Each branch $j \in \{1, 2, \ldots b_i\}$ in the range of f_i corresponds to an outgoing edge of the internal node. The leaf nodes in a decision tree are labeled by L. Figure 2a gives an example of a decision tree.

In order to represent (possibly partially constructed) decision trees at intermediate steps of our multi-objective search procedure, we consider a context-free grammar [17] $\mathfrak{G}$ that allows us to generate decision trees in a principled manner. Grammar $\mathfrak{G}$ uses the symbol N as the starting (non-terminal) symbol, and $\Sigma := \{\ [,\ ],\ ,\ ,\ f_1,\ f_2,\ \ldots f_{|F|},\ l_1,\ l_2,\ \ldots l_{|L|}\}$ as the set of terminal symbols. It has the following production rules:

$$N := f_1[\underbrace{N, N, \ldots N}_{b_1 \text{ times}}] \mid f_2[\underbrace{N, N, \ldots N}_{b_2 \text{ times}}] \mid \ldots \mid f_{|F|}[\underbrace{N, N, \ldots N}_{b_{|F|} \text{ times}}] \mid l_1 \mid l_2 \mid \ldots \mid l_{|L|}$$

We can imagine the start symbol as representing a (partially constructed) decision tree with a single node that is not yet labeled by a function from F or by a label from L. Every application of a production rule assigns a function f_i or a label l_j to an unlabeled node N. If a function f_i is assigned to an unlabeled node, then b_i outgoing edges are created, and b_i new unlabeled nodes are created, one for each new outgoing edge. We represent each function f_i in the grammar rules as $f_i[\underbrace{N, N, \ldots N}_{b_i \text{ times}}]$ to indicate that b_i new unlabeled nodes are created, one for each branch in the range of the function f_i. If a label l_j is assigned to an unlabeled node, no new nodes are created. We call decision trees containing unlabeled nodes as partial decision trees, and those not containing unlabeled nodes as complete decision trees. Figure 2b gives an example of a partial decision tree. Unless specified otherwise, by decision trees we will henceforth mean complete decision trees.

We now give the semantics of a decision tree: given an input $x \in \mathcal{I}$, a decision tree D outputs a label $l \in \mathcal{O}$, which we denote by $D(x)$, as per the following rules:

- if D is of the form $f_i[D_1, D_2, \ldots D_{b_i}]$ then $D(x) := D_{f_i(x)}(x)$
- if D is a leaf labeled l_j, then $D(x) := l_j$

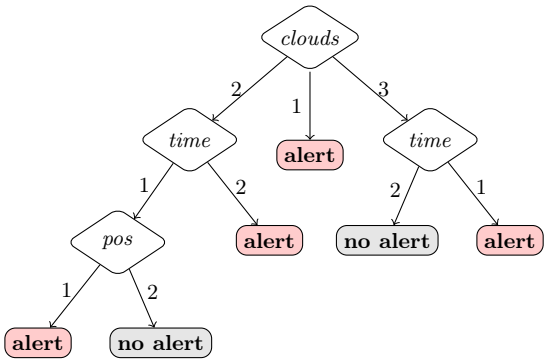

(a) Decision Tree with functions {*clouds*, *time*, *pos*} and labels {*alert*, *no alert*}. The functions *time* and *pos* have two outgoing branches, and *clouds* has tree.

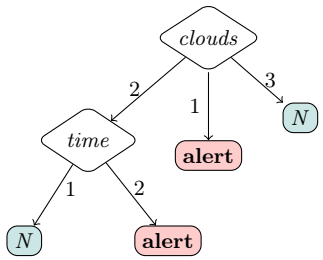

(b) Partial decision tree with two unassigned nodes labeled N be default.

Fig. 2: (a) Complete and (b) Partial Decision Tree

Note that $D_{f_i(x)}(x)$ is well defined since the range of f_i is $\{1, 2, \ldots b_i\}$.

As in [35], we assume that we have a node budget $B \in \mathbb{Z}_{>0}$ — a positive integer — that bounds the number of internal nodes in our decision trees. Thus, the class of interpretations $\mathcal{G}$ is restricted to decision trees generated by the grammar $\mathfrak{G}$ with at most B internal nodes. We denote the grammar with this restriction by $\mathfrak{G}_B$ and the corresponding class of interpretations by $\mathcal{G}_B$. Note, however, that the above is not a real restriction, since the number of semantically different decision trees for a finite set of features/predicates (represented by $f_i \in F$) and labels (represented by $l_j \in L$) is finite. To see this, observe that along any directed path $f_{i_1} \xrightarrow{b_{i_1}} f_{i_2} \xrightarrow{b_{i_1}} \ldots f_{i_j} \xrightarrow{b_{i_j}} \ldots f_{i_{k-1}} \xrightarrow{b_{i_{k-1}}} f_{i_k}$ in a decision tree, if there are two nodes with the same function $f_{i_j} = f_{i_k}$, then the second occurrence of f_{i_k} can be removed from the tree, by simply attaching the sub-tree rooted at the $b_{i_j}^{th}$ branch of f_{i_j} to the $b_{i_{k-1}}^{th}$ branch of $f_{i_{k-1}}$. It is easy to see that this doesn't change the semantics since any input $x \in \mathcal{I}$ evaluated along the path already evaluates to $f_{i_j}(x) = f_{i_k}(x) = b_{i_j}$. Therefore, there are only finitely many semantically different decision trees for a given set of functions and labels, and setting B to the maximum number of internal nodes in this set of semantically different trees allows us to include all semantically different decision trees in the class $\mathcal{G}_B$.

Explainability and Accuracy Measures We now define the explainability measure $\mathcal{E}$ and the correctness measure $\mathcal{C}$ on decision trees. Our correctness measure $\mathcal{C} : \mathcal{G}_B \to [0, 1]$ is a map from the set of decision trees to a number between 0 and 1. This gives the accuracy of the decision tree in predicting the output from an input, for samples drawn from the underlying distribution

$\Delta(\mathcal{I}\times\mathcal{O})$. That is, given a decision tree $D \in \mathcal{G}_B$, its correctness measure $\mathcal{C}(D) := \mathcal{P}_{(i,o)\sim\Delta(\mathcal{I}\times\mathcal{O})}[D(i) = o]$ is the probability of correctly classifying an input-output sample (i, o) from the distribution $\Delta(\mathcal{I} \times \mathcal{O})$. We estimate this measure using the Probably Approximately Correct (PAC) [30] framework, as done in [35]. Specifically, for a given tolerance ε and confidence $1 - \delta$, where $0 < \varepsilon, \delta < 1$, we first compute the sample complexity, say $\mu(\mathcal{G}, \varepsilon, \delta)$, of the finite class $\mathcal{G}_B$ of decision trees using standard techniques [30]. Then, we draw $\mu(\mathcal{G}, \varepsilon, \delta)$ i.i.d. samples of (input, output) values from the distribution $\Delta(\mathcal{I} \times \mathcal{O})$, and compute the fraction of times the output is correctly predicted by the decision tree D under consideration for these samples. PAC theory then guarantees that with probability at least $1 - \delta$, the computed estimate of the fraction lies within an additive tolerance of ε of the expected value of the fraction, when i.i.d. samples are drawn from the distribution $\Delta(\mathcal{I} \times \mathcal{O})$.

Our explainability measure $\mathcal{E} : \mathcal{G}_B \to \mathbb{R}_{>0}$ is a map from the set of decision trees to the set of positive real numbers. Below, we describe a specific explainability measure that assigns higher scores to small decision trees (typically, more explainable than large trees), and also to decision trees that use predicate/features that are more desirable to be included in an interpretation. Our overall approach is however not restricted to this specific explainability metric, and applies to any metric that can be encoded symbolically (see Section 4.2).

We assume that each function f_i has an associated (user-provided) weight $w_i \in \mathbb{Z}_+$, that gives us a measure of the desirability of including f_i in an interpretation. Higher weights represent functions that are more desirable to be included. Let $W := \max\limits_{1\le i\le|F|} w_i$ be the highest such weight. Given a decision tree D with m internal nodes containing i_1 nodes corresponding to the function f_1, i_2 nodes corresponding to f_2, ..., $i_{|F|}$ nodes corresponding to $f_{|F|}$, the explainability measure is given by $\mathcal{E}(D) := (B - m)|W + 1| + \sum\limits_{j=1}^{j=|F|} i_j * w_j$. That is, we first prioritize the unused nodes by giving them the highest weights. So, lower values of m correspond to more explainable the decision trees. This aligns with human intuition, that is, the smaller the decision tree, the easier it is to explain that decision tree. Then for a given size m, we prioritize the functions that are the most desirable to be included in an interpretation. This also aligns with human intuition as some functions may be difficult to explain than others.

4 A Two-Phase Algorithm: Search and Verification

Recall from our earlier discussion that our approach works in two phases. In the first phase, we use multi-objective Monte-Carlo Tree Search (MCTS) to solve a multi-objective optimization problem. Then, in the second phase we use SAT solvers to get local guarantees. In Section 4.1 we construct a Multi-Objective Markov Decision Process (MO-MDP). This MO-MDP has (partial or complete) decision trees as states, and uses actions that allow us to grow these decision trees. Then, we use Multi-Objective Monte-Carlo Tree Search [36] to search

through the MO-MDP to synthesize best-effort Pareto-optimal decision trees. Finally, we give local guarantees on the decision trees synthesized by the MO-MCTS using a Boolean satisfiability solver.

4.1 Multi-Objective MDP and MCTS

In this section, we model the generation of decision trees by the grammar $\mathfrak{G}_B$ as a deterministic MO-MDP, where each state corresponds to a (partial or complete) decision tree, and the production rules of $\mathfrak{G}_B$ determine the actions. Specifically, the transitions only have a probability of 0 or 1 depending on the current and next state. The probability is 1 for transitions that correspond to the production rule of the chosen action, and 0 otherwise. We then assign a multi-objective reward to the states, and apply MO-MCTS [36] to synthesize a best-effort approximation to the Pareto-optimal front.

Definition 3 (Multi-objective MDP). *A MO-MDP $M := (S, A, T, s_0, R)$ is a tuple, where S is a set of states, A is the set of actions, $T : S \times A \times S \to [0, 1]$ is the transition probability, s_0 is the initial state, and $R : S \times A \times S \to \mathbb{R}^2_{\geq 0}$ is a **two-dimensional vector-valued reward**.*

We assume that we are given a set $F := \{f_1, f_2, \dots f_{|F|}\}$ of functions, a set $L := \{l_1, l_2, \dots l_{|L|}\}$ of labels, a budget B bounding the number of internal nodes, and the grammar $\mathfrak{G}_B$ as defined in Section 2. We define the following deterministic MO-MDP $M_{\mathfrak{G}_B}$, where:

- Set of states $S := \{\alpha \mid N \overset{*}{\Rightarrow}_{\mathfrak{G}_B} \alpha\}$ is the set of all (partial or complete) decision trees generated by the application of zero or more rules from the grammar $\mathfrak{G}_B$ on the initial symbol N.
- The initial state s_0: $s_0 = N$ is the initial string N, which represents a partial decision tree with just one node corresponding to the non-terminal N.
- Set of actions A: $A := \{(i, j) \mid 1 \leq i \leq N_{max}$ and $1 \leq j \leq |F| + |L|\}$ is the set of all actions. Here N_{max} is the maximum number of non-terminals of a decision tree in the set $\mathcal{G}_B$. Each action is a tuple (i, j) that represents the application of j^{th} production rule of $\mathfrak{G}_B$ on the i^{th} non-terminal node to generate the next (partial or complete) decision tree. If the number of non-terminals in the current decision tree is less than i, then the transition on this action loops to the same decision tree.
- Since we consider a deterministic MO-MDP, the transition on an action $a = (i, j)$ is just the application of j^{th} production rule of $\mathfrak{G}_B$ on the i^{th} non-terminal if it exists, otherwise the transition corresponding to the action just loops back. The transition probabilities are given by the following:

$$T((s, a = (i, j), s')) := \begin{cases} 1, & \text{if the number of non-terminals in } s \text{ is more than } i, \text{ and applying the } j^{th} \text{ production rule on } i^{th} \text{ non-terminal results in } s' \\ 1, & \text{if } s = s' \text{ and there are less than } i \text{ non-terminals in } s \\ 0, & \text{otherwise} \end{cases}$$

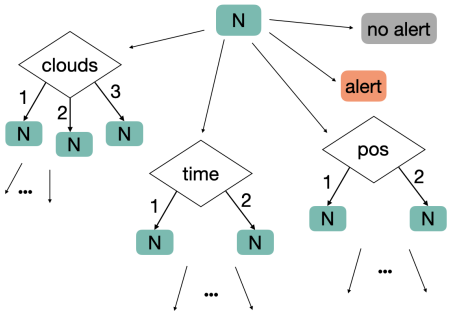

Fig. 3: Deterministic transitions in the MO-MDP

– A two-dimensional reward is given by the correctness measure in one dimension and the explainability measure in the other. For every transition (s, a, s') where s' is not a complete decision tree the reward is defined as $R((s, a, s')) := [0, 0]$. Otherwise, if s' is a complete decision tree, the reward is defined as $R((s, a, s')) := [\mathcal{C}(s'), \mathcal{E}(s')]$. i.e. the correctness and explainability measure of the (complete) decision tree s'. It is easy to see that we have a sparse setting for the reward.

Figure 3 shows some deterministic transitions from the initial node in an MO-MDP modeling one of our benchmarks (TaxiNet), where *clouds, time, pos* are elements of F, and *alert, noalert* are labels in L. The MO-MCTS algorithm developed in [36] works for deterministic MO-MDPs, and is therefore suitable use in our approach. The MO-MCTS procedure of [36] generates a search tree and maintains a set of best-effort approximations of Pareto-optimal interpretations over the search tree. This procedure has three phases. In the first phase, the procedure iteratively chooses an action until it arrives at a (search tree) node that has all unexplored actions, or until a Progressive Widening heuristic is triggered on a node with unexplored actions. This heuristic initially restricts the number of child nodes allowed for exploration. For each node, it only allows a limited number of child nodes for exploration at the start, and gradually increases this number as the visits to the parent node increase. This helps in managing the exploration initially by focusing on a smaller subset of actions. During the first phase, the actions chosen are those that maximize a quantity dependent on the hypervolume indicator [39] of the upper confidence bound, subtracted with an L_2-norm of the perspective projection of the upper confidence bound. Then it chooses an unexplored action using another heuristic that builds on the Rapid Action Value Estimation (RAVE) heuristic [14] by maximizing over all unexplored actions the L_2-norm of the difference between the perspective projection of the RAVE heuristic with itself. The second phase starts once an unexplored action is chosen. In this phase, the MO-MCTS procedure randomly selects actions until a terminal state is reached. Then in the third and final phase,

the multi-dimensional rewards are collected and the quantities required for the heuristics are updated by backtracking.

The MO-MCTS procedure maintains a set of best-effort approximations of Pareto-optimal interpretations that it keeps on improving in each iteration. Lemma 1 below quantifies this formally.

Lemma 1. *Let PO_i be an incomparable set of best-effort Pareto optimal points in the MO-MCTS procedure at iteration i. Then for every iteration $j > i$ and for every point $p \in PO_i$ there is a point $p' \in PO_j$ such that $p \preceq p'$.*

4.2 SAT Encoding

In this section, we describe the verification procedure for the interpretations obtained from the MO-MCTS procedure. We assume that the MO-MCTS procedure outputs a set $S := \{(D, \mathcal{C}(D), \mathcal{E}(E))\}$ of decision trees along with their correctness and explainability measures. Let δ_c and δ_e be the user-provided correctness and explainability slacks respectively. For each interpretation $(D, \mathcal{C}(D), \mathcal{D}(D))$ in S, this phase searches for an interpretation $D' \in \mathcal{G}_B$ s.t. $(\mathcal{C}(D) + \delta_c, \mathcal{E}(D) + \delta_e) \succeq (\mathcal{C}(D'), \mathcal{E}(D')) \succ (\mathcal{C}(D), \mathcal{E}(D))$ by encoding the problem as one of Boolean satisfiability, and by using a Boolean satisfiability solver. If it finds such a D', then it replaces D with D' in the set S, and repeats the above search using the satisfiability solver. Otherwise, it declares D as locally PO w.r.t δ_c and δ_e and moves it from S to a set S'. This phase also filters out the decision trees in S' that are already Pareto-dominated by other locally PO trees in S'. Thus, if allowed to run till completion, this phase computes a set S' of locally Pareto-optimal (w.r.t. δ_c and δ_e) decision trees that are Pareto-incomparable, such that each tree in S is either present in S' or is Pareto-dominated by a tree in S'.

To search for an interpretation D' satisfying $(\mathcal{C}(D) + \delta_c,\ \mathcal{E}(D) + \delta_e) \succeq (\mathcal{C}(D'),\ \mathcal{E}(D')) \succ (\mathcal{C}(D),\ \mathcal{E}(D))$, we use the encoding ideas in [35]. Specifically, we construct a Boolean formula $\Phi(X, Y, Z, W)$, where X, Y, Z, W are binary encodings of integers, that is satisfiable if and only if there is a decision tree $D' \in \mathcal{G}_B$ such that $(X, Y) \prec (\mathcal{C}(D'), \mathcal{E}(D')) \preceq (Z, W)$. Moreover, the formula is constructed such that the interpretation D' can be obtained directly from the satisfying assignment of Φ. Once Φ is obtained, we invoke a Boolean satisfiability solver on $\Phi(\mathcal{C}(D), \mathcal{E}(D), \mathcal{C}(D) + \delta_c, \mathcal{E}(D) + \delta_e)$ to find the desired D'. If the formula is unsatisfiable, then we know that D is LPO w.r.t δ_c and δ_e.

Motivated by the encoding ideas in [35], we obtain the formula $\Phi(X, Y, Z, W)$ is as a conjunction of four sub-formulas

$$\Phi(X, Y, Z, W) := \Phi_{syntax} \wedge \Phi_{corr}(X, Z) \wedge \Phi_{exp}(Y, W) \wedge \Phi(X, Y).$$

Here, Φ_{syntax} encodes a syntactic restriction that allows only those decision trees generated by the grammar $\mathfrak{G}_B$. Similarly, $\Phi_{corr}(X, Z)$ encodes a correctness restriction that is satisfiable if there is a decision tree D' such that $X \leq \mathcal{C}(D') \leq Z$. The formula $\Phi_{exp}(Y, W)$ is s.t. it is satisfiable iff there is a decision tree D such that $Y \leq \mathcal{E}(D) \leq W$. Finally, the fourth component $\Phi(X, Y)$ is satisfiable iff there is a decision tree D such that the correctness and explainability measures

dominate (X, Y), i.e., $(X, Y) \prec (\mathcal{C}(D'), \mathcal{E}(D'))$. We explain the encoding in more detail in Appendix A. The correctness of the encoding is formalized below.

Lemma 2. *There is a Boolean formula $\Phi(c, e, c+\delta_c, e+\delta_e)$ that is satisfiable if and only if there is a decision tree $D' \in \mathcal{G}_B$ such that $(c, e) \prec (\mathcal{C}(D'), \mathcal{E}(D')) \preceq (c+\delta_c, e+\delta_e)$.*

4.3 Overall Procedure

We now integrate the ideas in the previous two sections to come up with an anytime two-phase algorithm. Algorithm 1 takes as input the timeout $T_{\text{MO-MCTS}}$ of the first phase involving MO-MCTS, the overall timeout T_{overall}, and the slacks δ_c and δ_e. The algorithm runs in two phases. In the first phase, it executes the MO-MCTS procedure with a timeout $T_{\text{MO-MCTS}}$. Since MO-MCTS always maintains a set of best-effort Pareto-optimal points internally, we collect all these best-effort solutions in a set S once the time budget $T_{\text{MO-MCTS}}$ is exhausted. Specifically, we assume that at the end of the first phase, each element in set S is a decision tree $D \in \mathcal{G}_B$ along with the tuple $(\mathcal{C}(D), \mathcal{E}(D))$.

In the second phase, Algorithm 1 maintains a set S' of confirmed locally Pareto-optimal interpretations, and initializes S' to the empty set. It then iterates through each tree D in S, and invokes the `Check_SAT` function on the Boolean formula $\Phi(\mathcal{C}(D), \mathcal{E}(D), \mathcal{C}(D)+\delta_c, \mathcal{E}(D)+\delta_e)$. Function `Check_SAT` checks if the formula fed to it as input is satisfiable. If so, it returns a decision tree D', along with $(\mathcal{C}(D'), \mathcal{E}(D'))$ such that $(\mathcal{C}(D), \mathcal{E}(D)) \prec (\mathcal{C}(D'), \mathcal{E}(D')) \preceq (\mathcal{C}(D) + \delta_c, \mathcal{E}(D)+\delta_e)$. Since D' Pareto-dominates D, we replace the entry $(D, (\mathcal{C}(D), \mathcal{E}(D)))$ in S by $(D', (\mathcal{C}'(D), \mathcal{E}(D')))$. If, on the other hand, `Check_SAT` reports that $\Phi(\mathcal{C}(D), \mathcal{E}(D), \mathcal{C}(D) + \delta_c, \mathcal{E}(D) + \delta_e)$ is unsatisfiable, we know that D is LPO w.r.t. δ_c and δ_e, and add $(C, (\mathcal{C}(D), \mathcal{E}(D)))$ to the set S', while ensuring that no two interpretations in S' Pareto-dominate each other. If the overall timeout T_{overall} is exceeded while `Check_SAT` is in execution, we assume that `Check_SAT` is forcibly terminated and the status returned indicates timeout. In such cases, we retain $(D, (\mathcal{C}(D), \mathcal{E}(D)))$ in the set S.

The second phase of Algorithm 1 iterates until the overall timeout T_{overall} is reached or the set S becomes empty. In either case, the algorithm returns the sets S' and S, with the guarantee that S' contains incomparable LPO interpretations w.r.t. δ_c and δ_e. The interpretations in S, however, are simply best-effort interpretations that may not be LPO w.r.t. δ_c and δ_e.

Theorem 1. *Suppose Algorithm 1 outputs sets S' and S of decision trees along with their associated measures on termination. Then, every decision tree D in S' is LPO w.r.t. δ_c and δ_e. Furthermore, for every decision tree D in S, there exists at least one tree D' output by MO-MCTS s.t. $(\mathcal{C}(D'), \mathcal{E}(D')) \preceq (\mathcal{C}(D), \mathcal{E}(D))$.*

Note that Theorem 1 holds regardless of whether Algorithm 1 terminates due to S becoming empty or T_{overall} being exceeded. It is also easy to verify that Algorithm 1 is guaranteed to output at least one decision tree (in either S or S') if the first phase of MO-MCTS does not return an empty set. This suggests the following corollary.

Algorithm 1: Anytime LPO Interpretation Synthesis

Input: Timeouts $T_{\text{MO-MCTS}}$ and T_{overall} of MO-MCTS and overall algorithm
Slack δc of correctness measure $\mathcal{C}$
Slack δe of explainability measure $\mathcal{E}$

Output: Set S' of incomparable interpretations that are LPO w.r.t. δc and δe
Set S of best-effort interpretations

`/* Execute the first phase of MO-MCTS */`
$S \leftarrow$ `execute_with_timeout`(MO-MCTS, $T_{\text{MO-MCTS}}$)

`/* Execute the second phase of verification */`
$S' \leftarrow \{\}$

while $S \neq \emptyset$ *or* $T_{overall}$ *not exceeded* **do**

  $(D, (c, e)) \leftarrow S.pop()$ `// fetch and remove an element` $D, (c, e)$ `from` S

  (status, assignment) = `Check_SAT`($\Phi(c, e, c + \delta_c, e + \delta_e), T_{\text{overall}}$)
  if *status is unsatisfiable* **then**
    $S' \leftarrow S' \cup \{(D, (c, e))\}$
    Remove Pareto-dominated interpretations from S'
  else if *status is satisfiable* **then**
    `/* the satisfying assignment encodes a decision tree` D' `with measures` (c', e') `s.t.` $(c, e) \prec (c', e') \preceq (c + \delta_c, e + \delta_e)$ `*/`
    $(D', (c', e')) \leftarrow$ extract_decision_tree(assignment)
    $S \leftarrow S \cup \{(D', (c', e'))\}$
    Remove Pareto-dominated interpretations from S
  else
    `/*` $T_{\texttt{overall}}$ `exceeded during Check_SAT call */`
    $S \leftarrow S \cup \{(D, (c, e))\}$

return S' *and* S

Corollary 1. *With sufficiently large overall timeout $T_{overall}$ and with sufficiently large values of δ_c and δ_e, Algorithm 1 is guaranteed to find at least one PO interpretation.*

5 Experiments

We have implemented the MO-MCTS procedure of [36] adapted to our setting, and the verification algorithm described above in a prototype tool called ALPO available at https://github.com/anirjoshi/ALPO. All our experiments were run on an Apple Mac M2 Pro with 32 GB memory. In the experiments, we set the timeout $T_{\text{MO-MCTS}}$ for MO-MCTS to be exactly half of the overall timeout T_{overall}. We experimented with two different values of the overall timeout T_{overall}, viz. 5 mins and 20 mins. We used the Kissat SAT solver [7] to solve the Boolean

satisfiability queries in the verification phase of Algorithm 1. In the first phase involving MO-MCTS, we restricted the actions of MO-MDP to only allow those actions that involve the first non-terminal. Without this restriction, we empirically observed that the action set becomes very large. We also note that the restriction does not reduce the expressivity, as the actions may be applied in any order. For example, in Figure 2b, actions for any of the two non-terminals can be taken first. This restriction just enforces an ordering on the actions by always selecting an action corresponding to the first non-terminal.

For each state, we also skipped explore the self-looping actions, since they do not contribute towards exploration. Finally, from the initial state of the MO-MDP we do not allow actions involving labels in the set L, since allowing such actions would give rise to single-node decision trees that classify every input to the same label. We compare our work with the tool Synplicate developed as part of [35], which is guaranteed to synthesize the full Pareto-optimal curve of interpretations, when it does terminate (which as we show is not always the case). Since Synplicate considers interpretations as decision diagrams, we modified it slightly to restrict the interpretations to decision trees. We used the same timeout T_{overall} for Synplicate as used by ALPO.

Benchmarks For our benchmarks, we considered a set of 10 benchmarks from the UCI repository [23], 3 custom-made benchmarks, and 5 randomly generated benchmarks. In this section, we present the four most relevant benchmarks namely AutoTaxi, Balance Scale [31], Car Evaluation [8] and Yeast [25]. The remaining are detailed in Appendix B.

All of our benchmarks have categorical outputs. The AutoTaxi benchmark, adapted from [13,34], is a decision module that predicts whether a perception module of an airplane behaves correctly under certain environment conditions. It uses the following features: time of day, types of clouds, and initial position of the airplane on the runway. The implementation of this module is a decision tree based on data collected from 200 simulations, using the XPlane (`https://www.x-plane.com`) simulator.

The other benchmarks Balance Scale, Car Evaluation, and Yeast are all collected from the UCI Machine Learning Repository [23]. These benchmarks are available as datasets. We first train these datasets on a fully connected neural network with four hidden layers containing seven neurons in each layer, and a ReLU activation function for each neuron. This neural network then serves as our black-box model. For the synthesis procedure, we restrict the space of decision trees to only those with size less than six internal nodes. The names of functions for the decision tree are the same as the names of features in the dataset. For every categorical feature, we assign a number to each category, and the feature function in the decision tree just outputs the number according to the category. For every numerical feature $\mathbf{f}$, we have a function f that has three output buckets. This function simply divides the range of the feature into three equal regions. Let $\mathbf{f}_{max}$ and $\mathbf{f}_{min}$ be the maximum and minimum values of $\mathbf{f}$ in

Benchmark Name	Features	Weights	Output Branches
AutoTaxi	clouds, day time, init pos	1, 4, 3	6, 3, 4
Balance Scale	left distance, left weight	3, 3	3, 3
	right distance, right weight	3, 3	3, 3
Car Evaluation	buying, doors, lug boot	3, 3, 3	4, 4, 3
	maint, persons, safety	3, 3, 3	4, 3, 3
Yeast	alm, erl, gvh, mcg, mit	3, 3, 3, 3	3, 3, 3, 3
	nuc, pox, vac	3, 3, 3	3, 3, 3

Table 1: List of feature names, weights and output branches in all benchmarks

the dataset. Then $f\colon \mathbb{R} \to \{0, 1, 2\}$ is defined as:

$$f(i) := \begin{cases} 0, & \text{if } i < \mathbf{f}_{min} + \frac{\mathbf{f}_{max} - \mathbf{f}_{min}}{3} \\ 1, & \text{else if } i < \mathbf{f}_{min} + 2 * \frac{\mathbf{f}_{max} - \mathbf{f}_{min}}{3} \\ 2, & \text{otherwise} \end{cases}$$

In Table 1, we list the features used in these four benchmarks. We plot the results of executing ALPO and Synplicate on these benchmarks in Figure 6. We first discuss the results with an overall timeout of 20 minutes. (10 mins for MO-MCTS, and 10 mins for the second phase in ALPO). The (δ_c, δ_e) windows for AutoTaxi, Car Evaluation, Balance Scale, and Yeast are $(0.023, 5)$, $(0.018, 5)$, $(0.021, 5)$ and $(0.017, 5)$, respectively. The δ_c values are obtained as $\frac{10}{K}$, where K is the total number of samples used for a benchmark. We use $\epsilon = 0.25$ and $\delta = 0.1$ for the PAC guarantees, without making any realizability assumption.

The research questions We address the following three research questions.

- RQ1: Are locally Pareto-optimal solutions given by our approach close to the actual (global) Pareto-optimal solutions?
- RQ2: Does the MO-MCTS procedure output a good approximation of the Pareto-optimal curve?
- RQ3: Does our procedure scale empirically in comparison with Synplicate?

5.1 Our Results

RQ1: From local Pareto-optimality to global Pareto-optimality. Our experiments reveal that the search for locally Pareto-optimal solutions around the solutions of the MO-MCTS procedure often gives us globally Pareto-optimal solutions. We use the AutoTaxi and the Balance Scale benchmarks to demonstrate this. Indeed, these are the only benchmarks (among the four being discussed here) where the Synplicate tool terminates within 20 mins, and hence gives the Pareto-optimal curve, allowing us to perform this comparison.

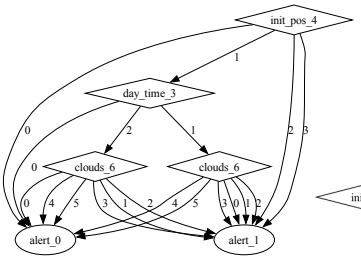

Fig. 4: Decision tree corresponding to point P in Figure 6a from the first phase of MO-MCTS with correctness and explainability measures 0.916 and 14 respectively.

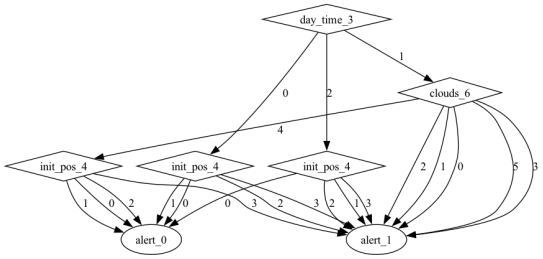

Fig. 5: Decision tree corresponding to point Q from the second phase of verification procedure with correctness and explainability 0.918 and 14 resp.

In the AutoTaxi benchmark, we observe from the Pareto-optimal curve in Figure 6a that all decision trees except one [P=(0.916,14)] from the MO-MCTS procedure are Pareto-optimal. Also, we are able to discover a Pareto-optimal decision tree Q close to P = (0.916, 14) in the second phase. We show the decision trees representing points P and Q in Figures 4 and 5 respectively.

RQ2: MO-MCTS is a good approximation of the Pareto-optimal curve The plots in Figure 6a and Figure 6b corresponding to the AutoTaxi and Balance Scale benchmarks, respectively, provide evidence that the MO-MCTS procedure gives a good approximation of the (actual) Pareto-optimal curve, as given by Synplicate. The MO-MCTS procedure outputs eight of the combined twelve Pareto-optimal points. We cannot use the other two benchmarks to answer this question, because the Synplicate tool times out before outputting even one Pareto-optimal point.

RQ3: Performance of ALPO vs Synplicate Finally, we address whether our procedure performs better than Synplicate on a wider set of benchmarks. We answer this affirmatively by looking into the two benchmarks: Car Evaluation and Yeast. More evidence is presented in Appendix B via other benchmarks. As can be observed from the results of the Car Evaluation benchmark in Figure 6c and the Yeast benchmark in Figure 6d, the Synplicate tool cannot output even a single Pareto-optimal point for these benchmarks. Since the number of feature nodes in these benchmarks is more than those of the other two, this increases the size of the search space significantly. We believe this eventually causes Synplicate to choke. However, ALPO outputs at least four decision trees for each benchmark. Figure 7 shows the decision tree correponding to highest accuracy decision tree synthesized by this approach. Moreover, for each of the two benchmarks, we are able to verify that two decision trees are locally Pareto-optimal. Therefore, using our procedure, we are able to synthesize locally Pareto-optimal decision trees even in the cases where synthesizing a Pareto-optimal set is practically computationally intensive.

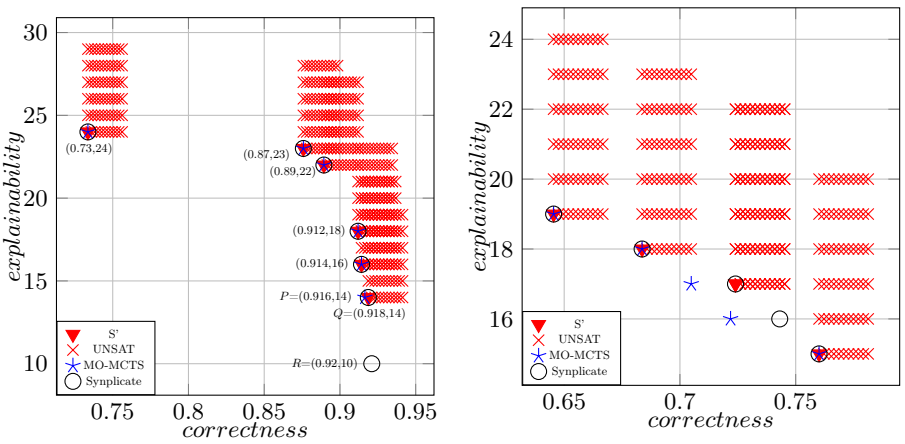

(a) AutoTaxi [35] (b) Balance Scale [31]

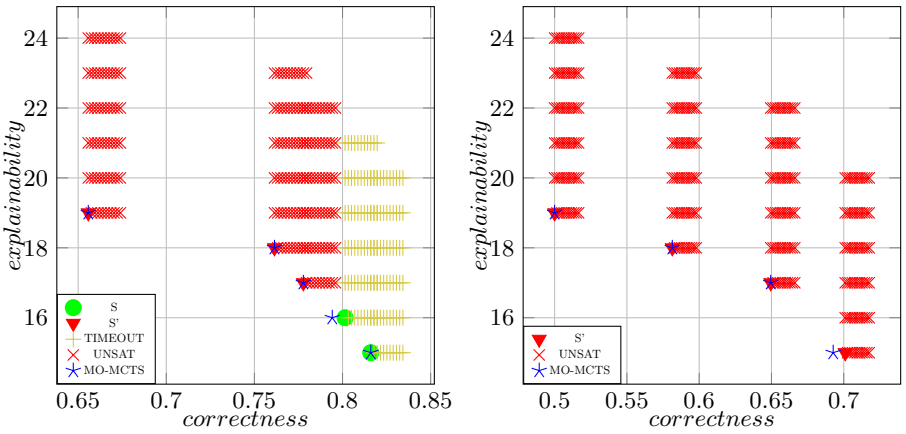

(c) Car Evaluation [8] (d) Yeast [25]

Fig. 6: Visualization of results: For each benchmark, correctness measure is plotted on X-axis and explainability measure on Y-axis. Blue stars indicate MO-MCTS results. Red inverted triangle indicate LPO interpretations found by ALPO. Red crosses indicate absence of interpretations with corresponding explainability-accuracy measures. Green solid circles indicate points that dominate an interpretation obtained from MO-MCTS, but not verified to be LPO. Yellow pluses indicate that ALPO timed out when checking for LPO here. Synplicate results are shown with hollow circles.

In summary, our results answer RQ1-3 comprehensively and show the effectiveness of ALPO. We also conducted experiments on several other benchmarks (see Appendix B), and repeated the experiments on the four benchmarks presented above with a 5 mins timeout (see Appendix C).

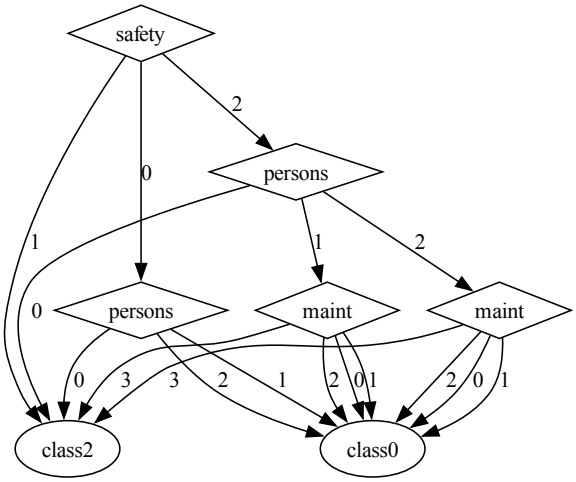

Fig. 7: Decision tree corresponding to the most accurate best-effort Pareto-point from the MO-MCTS for Car Evaluation benchmark.

Our results consistently support the conclusions w.r.t. RQ1-3 made above. In particular, when running with timeout of 5 mins, ALPO gives fewer (but non-empty) LPO interpretations than with 20 mins timeout, and hence degrades gracefully. This shows the value of ALPO as an anytime LPO interpretation synthesis algorithm.

6 Conclusion

In this paper, we have considered an integrated multi-objective MCTS-based search algorithm with SAT-based verification to synthesize Pareto-optimal interpretations with locally optimality guarantees. Our experimental results show that the interpretations we generate are close to globally Pareto-optimal illustrating the practical significance of the approach. As future work, it would be interesting to use the solutions from the SAT solver to improve search, leading to even better integration between these approaches. Future advancements in methods for MCTS-based search will directly transfer to our approach.

References

1. National Poll on Healthy Aging (NPHA). UCI Machine Learning Repository (2017), DOI: https://doi.org/10.3886/ICPSR37305.v1
2. Early Stage Diabetes Risk Prediction. UCI Machine Learning Repository (2020), DOI: https://doi.org/10.24432/C5VG8H
3. Heart Failure Clinical Records. UCI Machine Learning Repository (2020), DOI: https://doi.org/10.24432/C5Z89R
4. Adadi, A., Berrada, M.: Peeking inside the black-box: A survey on explainable artificial intelligence (XAI). IEEE Access **6**, 52138–52160 (2018). https://doi.org/10.1109/ACCESS.2018.2870052, https://doi.org/10.1109/ACCESS.2018.2870052
5. Aha, D.: Tic-Tac-Toe Endgame. UCI Machine Learning Repository (1991), DOI: https://doi.org/10.24432/C5688J
6. Andras, J., William, S., Pfisterer, M., Detrano, R.: Heart Disease. UCI Machine Learning Repository (1989), DOI: https://doi.org/10.24432/C52P4X
7. Biere, A., Faller, T., Fazekas, K., Fleury, M., Froleyks, N., Pollitt, F.: CaDiCaL, Gimsatul, IsaSAT and Kissat entering the SAT Competition 2024. In: Heule, M., Iser, M., Järvisalo, M., Suda, M. (eds.) Proc. of SAT Competition 2024 – Solver, Benchmark and Proof Checker Descriptions. Department of Computer Science Report Series B, vol. B-2024-1, pp. 8–10. University of Helsinki (2024)
8. Bohanec, M.: Car Evaluation. UCI Machine Learning Repository (1988), DOI: https://doi.org/10.24432/C5JP48
9. Browne, C., Powley, E.J., Whitehouse, D., Lucas, S.M., Cowling, P.I., Rohlfshagen, P., Tavener, S., Liebana, D.P., Samothrakis, S., Colton, S.: A survey of monte carlo tree search methods. IEEE Trans. Comput. Intell. AI Games **4**(1), 1–43 (2012)
10. Charalampakos, F., Tsouparopoulos, T., Koutsopoulos, I.: Joint explainability-performance optimization with surrogate models for ai-driven edge services (2025), https://arxiv.org/abs/2503.07784
11. Chen, W., Liu, L.: Pareto monte carlo tree search for multi-objective informative planning. CoRR **abs/2111.01825** (2021)
12. Craven, M.W., Shavlik, J.W.: Extracting tree-structured representations of trained networks. In: Touretzky, D.S., Mozer, M., Hasselmo, M.E. (eds.) Advances in Neural Information Processing Systems 8, NIPS, Denver, CO, USA, November 27-30, 1995. pp. 24–30. MIT Press (1995), http://papers.nips.cc/paper/1152-extracting-tree-structured-representations-of-trained-networks
13. Fremont, D.J., Chiu, J., Margineantu, D.D., Osipychev, D., Seshia, S.A.: Formal analysis and redesign of a neural network-based aircraft taxiing system with verifai. In: CAV (1). Lecture Notes in Computer Science, vol. 12224, pp. 122–134. Springer (2020)
14. Gelly, S., Silver, D.: Combining online and offline knowledge in UCT. In: ICML. ACM International Conference Proceeding Series, vol. 227, pp. 273–280. ACM (2007)
15. Guidotti, R., Monreale, A., Ruggieri, S., Pedreschi, D., Turini, F., Giannotti, F.: Local rule-based explanations of black box decision systems. CoRR **abs/1805.10820** (2018), http://arxiv.org/abs/1805.10820
16. Guidotti, R., Monreale, A., Ruggieri, S., Turini, F., Giannotti, F., Pedreschi, D.: A survey of methods for explaining black box models. ACM Comput. Surv. **51**(5), 93:1–93:42 (2019). https://doi.org/10.1145/3236009, https://doi.org/10.1145/3236009

17. Hopcroft, J.E., Ullman, J.D.: Introduction to Automata Theory, Languages and Computation. Addison-Wesley (1979)
18. Johansson, U., König, R., Löfström, T., Boström, H.: Evolved decision trees as conformal predictors. In: Proceedings of the IEEE Congress on Evolutionary Computation, CEC 2013, Cancun, Mexico, June 20-23, 2013. pp. 1794–1801. IEEE (2013). https://doi.org/10.1109/CEC.2013.6557778, https://doi.org/10.1109/CEC.2013.6557778
19. Krishnan, R., Sivakumar, G., Bhattacharya, P.: Extracting decision trees from trained neural networks. Pattern Recognit. **32**(12), 1999–2009 (1999). https://doi.org/10.1016/S0031-3203(98)00181-2, https://doi.org/10.1016/S0031-3203(98)00181-2
20. Krishnan, S., Wu, E.: PALM: machine learning explanations for iterative debugging. In: Binnig, C., Hellerstein, J.M., Parameswaran, A.G. (eds.) Proceedings of the 2nd Workshop on Human-In-the-Loop Data Analytics, HILDA@SIGMOD 2017, Chicago, IL, USA, May 14, 2017. pp. 4:1–4:6. ACM (2017). https://doi.org/10.1145/3077257.3077271, https://doi.org/10.1145/3077257.3077271
21. Luc, D.T.: Pareto Optimality, pp. 481–515. Springer New York, New York, NY (2008)
22. Lundberg, S.M., Lee, S.: A unified approach to interpreting model predictions. In: Guyon, I., von Luxburg, U., Bengio, S., Wallach, H.M., Fergus, R., Vishwanathan, S.V.N., Garnett, R. (eds.) Advances in Neural Information Processing Systems 30: Annual Conference on Neural Information Processing Systems 2017, December 4-9, 2017, Long Beach, CA, USA. pp. 4765–4774 (2017), https://proceedings.neurips.cc/paper/2017/hash/8a20a8621978632d76c43dfd28b67767-Abstract.html
23. Markelle Kelly, Rachel Longjohn, K.N.: The UCI Machine Learning Repository, https://archive.ics.uci.edu
24. Nakai, K.: Ecoli. UCI Machine Learning Repository (1996), DOI: https://doi.org/10.24432/C5388M
25. Nakai, K.: Yeast. UCI Machine Learning Repository (1991), DOI: https://doi.org/10.24432/C5KG68
26. Nakai, K.: Yeast. UCI Machine Learning Repository (1991), DOI: https://doi.org/10.24432/C5KG68
27. Quinlan, J.: Credit Approval. UCI Machine Learning Repository (1987), DOI: https://doi.org/10.24432/C5FS30
28. Ribeiro, M.T., Singh, S., Guestrin, C.: "why should I trust you?": Explaining the predictions of any classifier. In: Proceedings of the Demonstrations Session, NAACL HLT 2016, The 2016 Conference of the North American Chapter of the Association for Computational Linguistics: Human Language Technologies, San Diego California, USA, June 12-17, 2016. pp. 97–101. The Association for Computational Linguistics (2016). https://doi.org/10.18653/V1/N16-3020, https://doi.org/10.18653/v1/n16-3020
29. Ribeiro, M.T., Singh, S., Guestrin, C.: Anchors: High-precision model-agnostic explanations. In: McIlraith, S.A., Weinberger, K.Q. (eds.) Proceedings of the Thirty-Second AAAI Conference on Artificial Intelligence, (AAAI-18), the 30th innovative Applications of Artificial Intelligence (IAAI-18), and the 8th AAAI Symposium on Educational Advances in Artificial Intelligence (EAAI-18), New Orleans, Louisiana, USA, February 2-7, 2018. pp. 1527–1535. AAAI Press (2018). https://doi.org/10.1609/AAAI.V32I1.11491, https://doi.org/10.1609/aaai.v32i1.11491
30. Shalev-Shwartz, S., Ben-David, S.: Understanding Machine Learning - From Theory to Algorithms. Cambridge University Press (2014)

31. Siegler, R.: Balance Scale. UCI Machine Learning Repository (1976), DOI: https://doi.org/10.24432/C5488X
32. Siegler, R.: Balance Scale. UCI Machine Learning Repository (1976), DOI: https://doi.org/10.24432/C5488X
33. Swiechowski, M., Godlewski, K., Sawicki, B., Mandziuk, J.: Monte carlo tree search: a review of recent modifications and applications. Artif. Intell. Rev. **56**(3), 2497–2562 (2023)
34. Torfah, H., Junges, S., Fremont, D.J., Seshia, S.A.: Formal analysis of ai-based autonomy: From modeling to runtime assurance. In: Feng, L., Fisman, D. (eds.) Runtime Verification - 21st International Conference, RV 2021, Virtual Event, October 11-14, 2021, Proceedings. Lecture Notes in Computer Science, vol. 12974, pp. 311–330. Springer (2021). https://doi.org/10.1007/978-3-030-88494-9_19, https://doi.org/10.1007/978-3-030-88494-9_19
35. Torfah, H., Shah, S., Chakraborty, S., Akshay, S., Seshia, S.A.: Synthesizing pareto-optimal interpretations for black-box models. In: FMCAD. pp. 153–162. IEEE (2021)
36. Wang, W., Sebag, M.: Multi-objective monte-carlo tree search. In: ACML. JMLR Proceedings, vol. 25, pp. 507–522. JMLR.org (2012)
37. Yu, J., Ignatiev, A., Stuckey, P.J., Bodic, P.L.: Computing optimal decision sets with SAT. In: Simonis, H. (ed.) Principles and Practice of Constraint Programming - 26th International Conference, CP 2020, Louvain-la-Neuve, Belgium, September 7-11, 2020, Proceedings. Lecture Notes in Computer Science, vol. 12333, pp. 952–970. Springer (2020). https://doi.org/10.1007/978-3-030-58475-7_55, https://doi.org/10.1007/978-3-030-58475-7_55
38. Zhang, R., Xin, R., Seltzer, M.I., Rudin, C.: Optimal sparse regression trees. In: Williams, B., Chen, Y., Neville, J. (eds.) Thirty-Seventh AAAI Conference on Artificial Intelligence, AAAI 2023, Thirty-Fifth Conference on Innovative Applications of Artificial Intelligence, IAAI 2023, Thirteenth Symposium on Educational Advances in Artificial Intelligence, EAAI 2023, Washington, DC, USA, February 7-14, 2023. pp. 11270–11279. AAAI Press (2023). https://doi.org/10.1609/AAAI.V37I9.26334, https://doi.org/10.1609/aaai.v37i9.26334
39. Zitzler, E., Thiele, L.: Multiobjective optimization using evolutionary algorithms - A comparative case study. In: PPSN. Lecture Notes in Computer Science, vol. 1498, pp. 292–304. Springer (1998)

A Verification using Boolean Satisfiability

We describe below the construction a boolean formula $\Phi(X, Y, Z, W)$ that is satisfiable if and only if there is a decision tree $D \in \mathcal{G}_B$ such that $(X, Y) \prec (\mathcal{C}(D), \mathcal{E}(D)) \preceq (Z, W)$. Specifically, we are interested in instances of the formula of the form $\Phi(c, e, c+\delta_c, e+\delta_e)$, where (c, e) gives the accuracy and explainability measure of a known decision tree, and δ_c, δ_e are user-provided slacks for accuracy and explainability respectively. We build on ideas for a similar encoding, used in [35].

We assume a set of functions $F := \{f_1, f_2, \ldots, f_{|F|} \mid f_i : \mathcal{I} \to \{1, 2, \ldots b_i\}\}$ for the decision tree and the set $L := \{l_1, l_2, \ldots l_{|L|}\}$ of labels. Let $b_{max} := \max_{1 \le i \le |F|} b_i$. We upper-bound the internal nodes by B. We will assume the correctness measure defined in Section 3.1, and assume $\mu(\mathcal{G}, \varepsilon, \delta)$ samples $M := \{(i, o) \mid \Delta(\mathcal{I} \times \mathcal{O})\}$

from the input-output distribution. For the explainability measure we assume a user-provided weight $w_i > 0$ with every function f_i, which determines the explainability of the function. We also assume that there exists a topological ordering over the nodes of every decision tree. It is fine if we do not know this ordering for every decision tree. Only the existence of an ordering will be used in the encoding.

The encoding for $\Phi(c, e, c + \delta_c, e + \delta_e)$ is a conjunction of four components

$$\Phi(c, e, c + \delta_c, e + \delta_e) := \Phi_{syntax} \wedge \Phi_{corr}(c, c + \delta_c) \wedge \Phi_{exp}(e, e + \delta_e) \wedge \Phi(c, e)$$

Φ_{syntax} As explained earlier, we modify the encoding from [35] to syntactically restrict the space to decision trees. We now describe the combined encoding:

We let the variable $\lambda_{i,p}$ encode that the i^{th} node in the decision tree is assigned a function p. Hence the number of such λ variables is $B \times |F|$. We first encode that each node is assigned to exactly one function. Let $E_i := \{\lambda_{i,p} \mid p \in F\}$, then

$$F_1 := \bigwedge_{1 \leq i \leq B} Exactly\_One(E_i)$$

where $Exactly\_One$ just encodes a boolean constraint that in every satisfying assignment exactly one of the variables in the set is true and all others are false. F_1 just encodes that every node is assigned to exactly one function.

We now let variable $\tau_{i,c,j}$ encode that the i^{th} node has an edge to the j^{th} node or the label j, labelled c. Since there is a topological ordering, we assume that $i < j$. There are $\frac{B \times (B-1)}{2} \times (b_{max} + |L|)$ such variables. We then create a sub-formula which encodes that from every node there is exactly one outgoing edge corresponding to every label. We let $E_{i,c} := \{\tau_{i,c,j} \mid i < j \leq B\}$

$$G_{i,c} := Exactly\_One(E_{i,c})$$

Then we encode the constraint that if a node is assigned a function, then exactly every outgoing edge has a unique label in the range of that function.

$$F_{i,p} := \lambda_{i,p} \rightarrow \Big(\bigwedge_{1 \leq c \leq b_p} G_{i,c} \Big) \wedge \Big(\bigwedge_{b_p < c \leq b_max} \neg \tau_{i,c,j} \Big)$$

Finally we conjoin this over all nodes and all functions:

$$F_2 := \bigwedge_{\substack{1 \leq i \leq B \\ p \in F}} F_{i,p}$$

Now, we restrict that every node must have at most one incoming edge. For this let $H_j := \{\tau_{i,c,j} \mid 1 \leq i < j,\ 1 \leq c \leq b_{max}\}$

$$F_3 := \bigwedge_{1 < j \leq B} At\_Most\_1(H_j)$$

$$\Phi_{syntax} := F_1 \wedge F_2 \wedge F_3$$

$\boldsymbol{\Phi_{corr}(c+\delta_c)}$ We now encode the leaves $m_{l,i}$ encodes that the i^{th} sample has output label l. We assign them True or False depending on if the label on the i^{th} sample is l

$$m_{l,i} := \begin{cases} T, & \text{if } o_i = l \\ F, & \text{otherwise} \end{cases}$$

Then we let the variable $m_{i,j}$ encode the constraint that the i^{th} node in the decision tree outputs correct label for the k^{th} sample correctly, and encode this constraint with the formula:

$$M_{i,k} := m_{i,k} \leftrightarrow \Big(\bigvee_{p \in F} \bigvee_{c \le b_p} \lambda_{i,p} \wedge func(M_k, p, c) \wedge \bigwedge_{\substack{j \in \{i+1,\ldots,B\} \cup \\ L}} (\tau_{i,c,j} \rightarrow m_{j,k)}) \Big)$$

where $func(M_k, p, c)$ is T iff the k^{th} sample outputs c on function p, i.e, $p(M_k) = c$. We do this for all samples and have the following

$$F_4 := \bigwedge_{\substack{1 \le i \le B \\ 1 \le k \le |M|}} M_{i,k}$$

We use the symbol C to denote $C := \sum_k m_{1,k}$

For bounding the correctness measure we use cardinality constraints on $m_{1,k}$ variables:

$$\Phi_{corr}(c, c+\delta_c) := Encode(C \le c + d_c) \wedge Encode(c \le C) \wedge F_4$$

$\boldsymbol{\Phi_{exp}(e+\delta_e)}$ We now encode the explainability constraints. Where we have a variable u_i which encodes that the i^{th} node is reachable from the initial node, and have the following constraint:

$$F_5 := u_1 \wedge \bigwedge_{2 \le i \le B} u_i \leftrightarrow \Big(\bigvee_{\substack{1 \le c \le c_{\max}, \\ 1 \le i' < i}} \tau_{i',c,i} \wedge u_{i'} \Big)$$

Then we have another variable $\overline{u_i}$ which encodes that the i^{th} node is not used

$$F_6 := \bigwedge_{1 \le i \le B} \neg u_i \leftrightarrow \overline{u_i}$$

Finally we also have a variable $\lambda'_{i,p}$ which encodes that the i^{th} node is used and has the function p assigned to it which we encode using the following formula:

$$F_7 := \bigwedge_{\substack{1 \le i \le B \\ p \in F}} \lambda'_{i,p} \leftrightarrow (\lambda_{i,p} \wedge u_i)$$

Let us use E to denote the term $E := \sum_{\substack{1 \le i \le B \\ p \in F}} w_p \lambda'_{i,p} + \sum_{1 \le i \le B} (W_{max} + 1)\overline{u_i}$

Now we encode the formula

$$\Phi(e, e+\delta_e) := F_5 \wedge F_6 \wedge F_7 \wedge Encode(E \le e + \delta_e) \wedge Encode(e \le E)$$

$\boldsymbol{\Phi(c, e)}$

$\Phi(c, e) := \big(Encode(e \leq E) \wedge Encode(c < C)\big) \vee \big(Encode(e < E) \wedge Encode(c \leq C)\big)$

B Extended Experiments

We present below comprehensive experimental results on all the benchmarks considered in our work. Only four of these were presented in the main paper due to lack of space. For all the experiments below, we used a total timeout of 20 mins (10 mins for MO-MCTS and 10 mins for the second phase of ALPO).

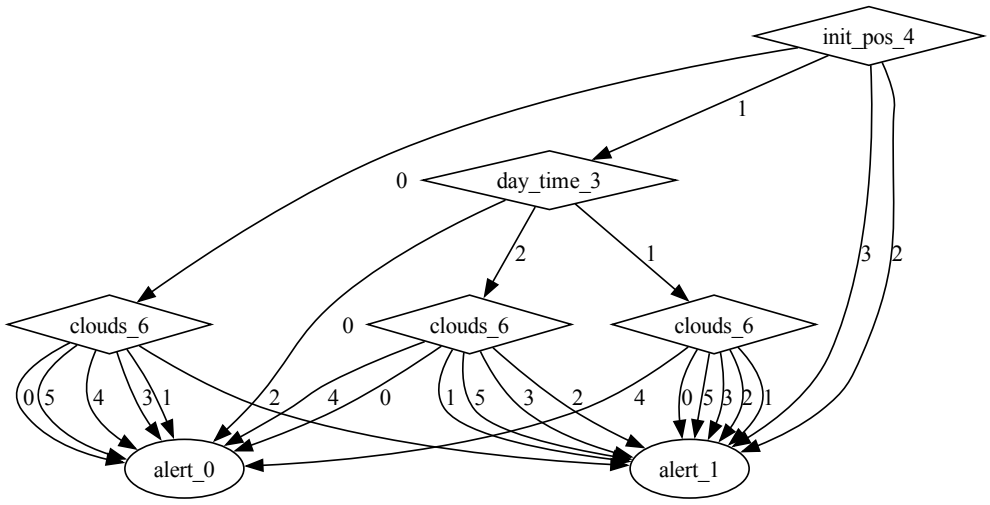

Fig. 8: Pareto-optimal decision tree with highest accuracy measure in the Auto-Taxi benchmark.

Feature Names	Weights	Output Branches
clouds_6	1	6
day_time_3	4	3
init_pos_4	3	4

Table 2: List of feature names, weights and output branches

AutoTaxi This represents the benchmark AutoTaxi. This is the same as presented in the main paper. We present the feature names, weights and partition in Table 21.

Figure 28 plots the results.

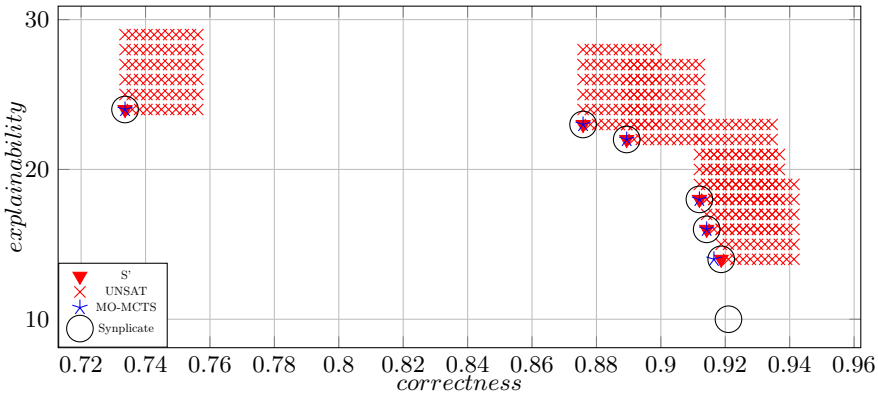

Fig. 9: AutoTaxi

Feature Names	Weights	Output Branches
left_distance	3	3
left_weight	3	3
right_distance	3	3
right_weight	3	3

Table 3: List of feature names, weights and output branches

balance scale This represents the benchmark balance scale. This is the same as presented in the main paper. We present the feature names, weights and partition in Table 22.

Figure 29 plots the results.

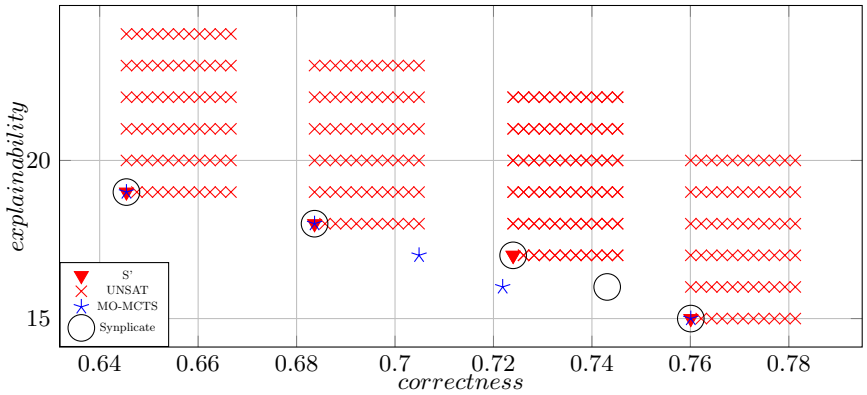

Fig. 10: balance scale

Feature Names	Weights	Output Branches
buying	3	4
doors	3	4
lug_boot	3	3
maint	3	4
persons	3	3
safety	3	3

Table 4: List of feature names, weights and output branches

car evaluation This represents the benchmark car evaluation. This is same as presented in the main paper. We present the feature names, weights and partition in Table 23.

Figure 30 plots the results.

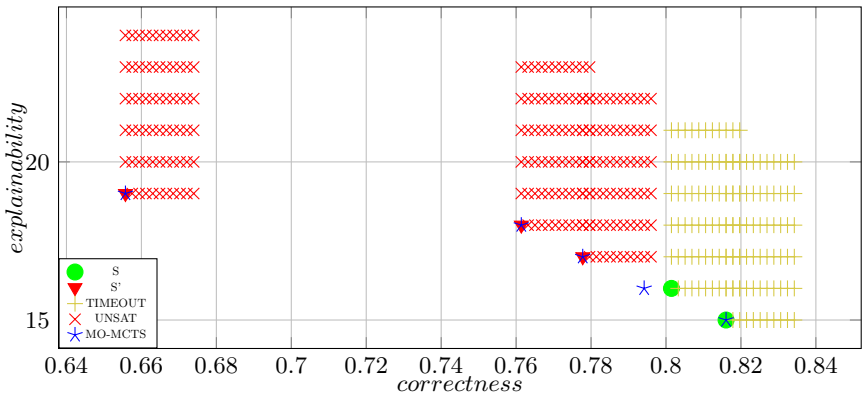

Fig. 11: car evaluation

Feature Names	Weights	Output Branches
aac	3	3
alm1	3	3
alm2	3	3
chg	3	3
gvh	3	3
lip	3	3
mcg	3	3

Table 5: List of feature names, weights and output branches

ecoli This represents the benchmark ecoli. This benchmark uses a neural network trained on the dataset [24] from the UCI repository. It restricts the space of decision trees to those with size at most 5. We present the feature names, weights and partition in Table 5.

Figure 12 plots the results.

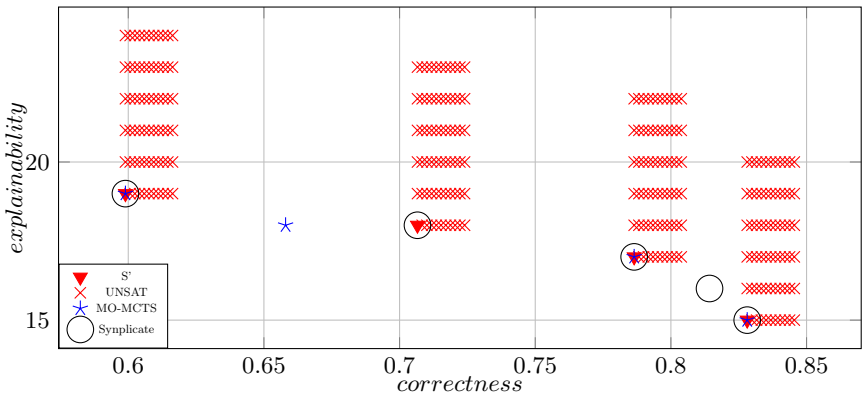

Fig. 12: ecoli

Feature Names	Weights	Output Branches
a10	3	2
a11	3	3
a12	3	2
a13	3	3
a15	3	3
a3	3	3
a8	3	3
a9	3	2

Table 6: List of feature names, weights and output branches

credit approval This represents the benchmark credit approval. This benchmark uses a neural network trained on the dataset [27] from the UCI repository. It restricts the space of decision trees to those with size at most 5. We present the feature names, weights and partition in Table 6.

Figure 13 plots the results.

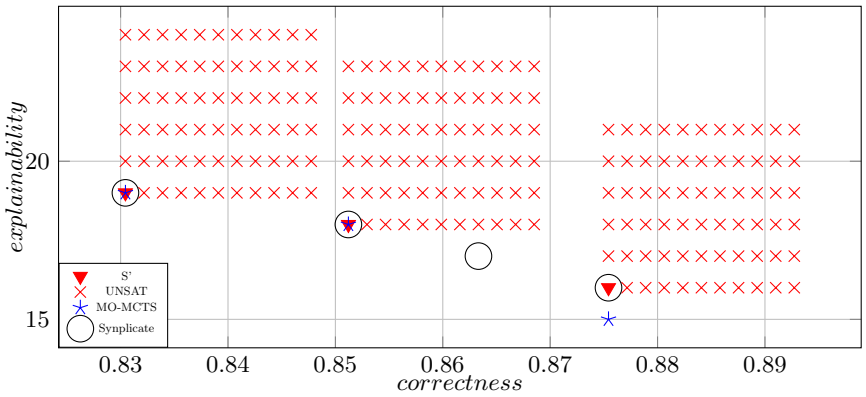

Fig. 13: credit approval

Feature Names	Weights	Output Branches
alm	3	3
erl	3	3
gvh	3	3
mcg	3	3
mit	3	3
nuc	3	3
pox	3	3
vac	3	3

Table 7: List of feature names, weights and output branches

yeast This represents the benchmark yeast. This benchmark uses a neural network trained on the dataset [25] from the UCI repository. It restricts the space of decision trees to those with size at most 5. We present the feature names, weights and partition in Table 24.

Figure 31 plots the results.

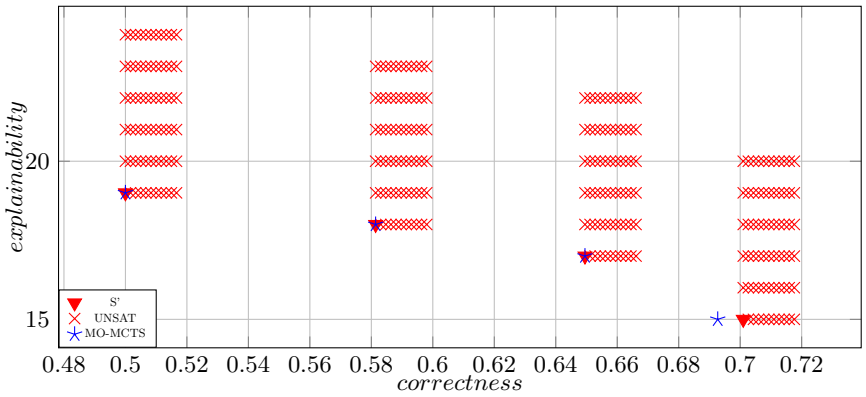

Fig. 14: yeast

Feature Names	Weights	Output Branches
bottom_left_square	3	3
bottom_middle_square	3	3
bottom_right_square	3	3
middle_left_square	3	3
middle_middle_square	3	3
middle_right_square	3	3
top_left_square	3	3
top_middle_square	3	3
top_right_square	3	3

Table 8: List of feature names, weights and output branches

tic tac toe endgame This represents the benchmark tic tac toe endgame. This benchmark uses a neural network trained on the dataset [5] from the UCI repository. It restricts the space of decision trees to those with size at most 5. We present the feature names, weights and partition in Table 8.

Figure 15 plots the results.

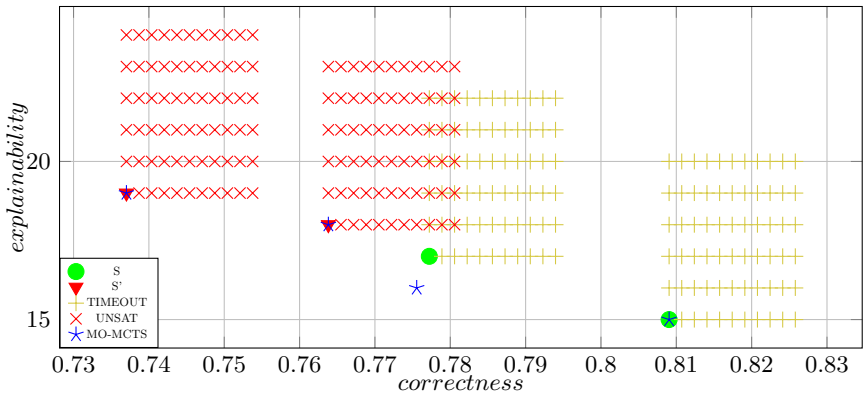

Fig. 15: tic tac toe endgame

Feature Names	Weights	Output Branches
age	3	3
chol	3	3
cp	3	3
exang	3	3
fbs	3	3
oldpeak	3	3
restecg	3	3
sex	3	3
slope	3	3
thalach	3	3
trestbps	3	3

Table 9: List of feature names, weights and output branches

heart disease This represents the benchmark heart disease. This benchmark uses a neural network trained on the dataset [6] from the UCI repository. It restricts the space of decision trees to those with size at most 5. We present the feature names, weights and partition in Table 9.

Figure 16 plots the results.

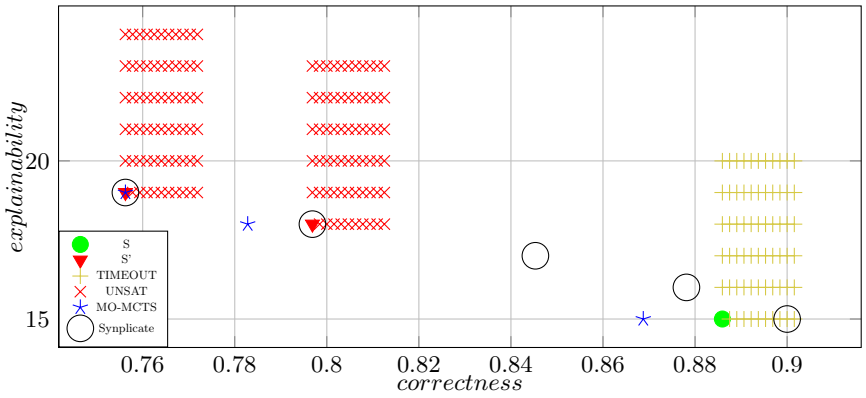

Fig. 16: heart disease

Feature Names	Weights	Output Branches
age	3	3
alopecia	3	2
delayed_healing	3	2
gender	3	2
genital_thrush	3	2
irritability	3	2
itching	3	2
muscle_stiffness	3	2
obesity	3	2
partial_paresis	3	2
polydipsia	3	2
polyphagia	3	2
polyuria	3	2
sudden_weight_loss	3	2
visual_blurring	3	2
weakness	3	2

Table 10: List of feature names, weights and output branches

early stage diabetes risk prediction This represents the benchmark early stage diabetes risk prediction. This benchmark uses a neural network trained on the dataset [2] from the UCI repository. It restricts the space of decision trees to those with size at most 5. We present the feature names, weights and partition in Table 10.

Figure 17 plots the results.

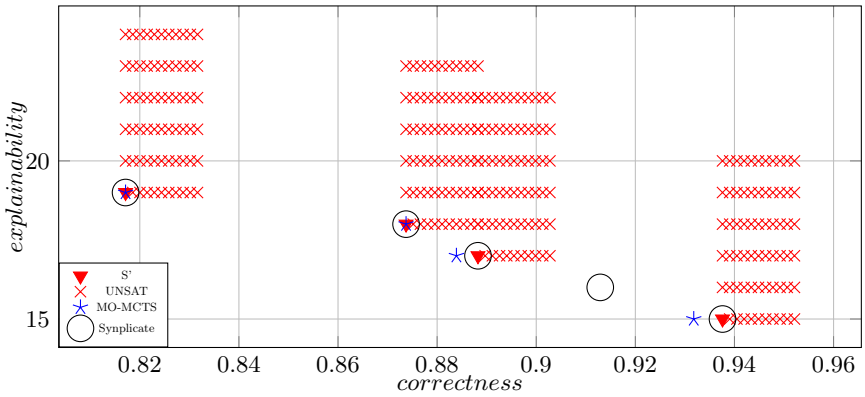

Fig. 17: early stage diabetes risk prediction

Feature Names	Weights	Output Branches
age	3	3
anaemia	3	3
creatinine_phosphokinase	3	3
diabetes	3	3
ejection_fraction	3	3
high_blood_pressure	3	3
platelets	3	3
serum_creatinine	3	3
serum_sodium	3	3
sex	3	3
smoking	3	3
time	3	3

Table 11: List of feature names, weights and output branches

heart failure clinical records This represents the benchmark heart failure clinical records. This benchmark uses a neural network trained on the dataset [3] from the UCI repository. It restricts the space of decision trees to those with size at most 5. We present the feature names, weights and partition in Table 11.

Figure 18 plots the results.

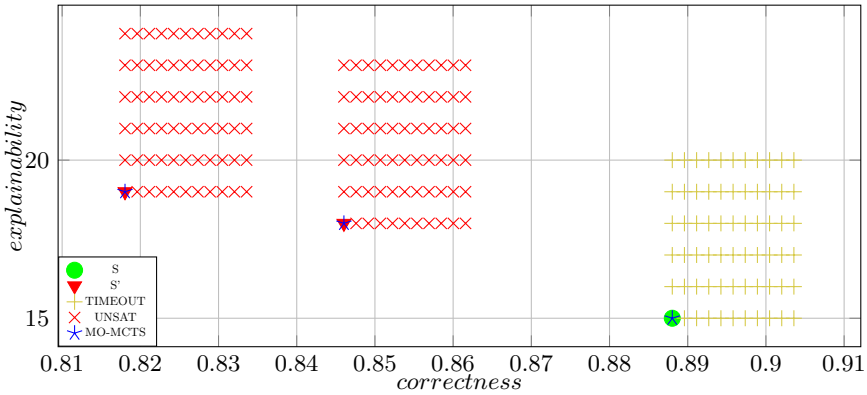

Fig. 18: heart failure clinical records

Feature Names	Weights	Output Branches
age	3	3
bathroom_needs_keeps_patient_from_sleeping	3	3
dental_health	3	3
employment	3	3
gender	3	3
medication_keeps_patient_from_sleeping	3	3
mental_health	3	3
pain_keeps_patient_from_sleeping	3	3
physical_health	3	3
prescription_sleep_medication	3	3
race	3	3
stress_keeps_patient_from_sleeping	3	3
trouble_sleeping	3	3
uknown_keeps_patient_from_sleeping	3	3

Table 12: List of feature names, weights and output branches

national poll on healthy aging npha This represents the benchmark national poll on healthy aging npha . This benchmark uses a neural network trained on the dataset [1] from the UCI repository. It restricts the space of decision trees to those with size at most 5. We present the feature names, weights and partition in Table 12.

Figure 19 plots the results.

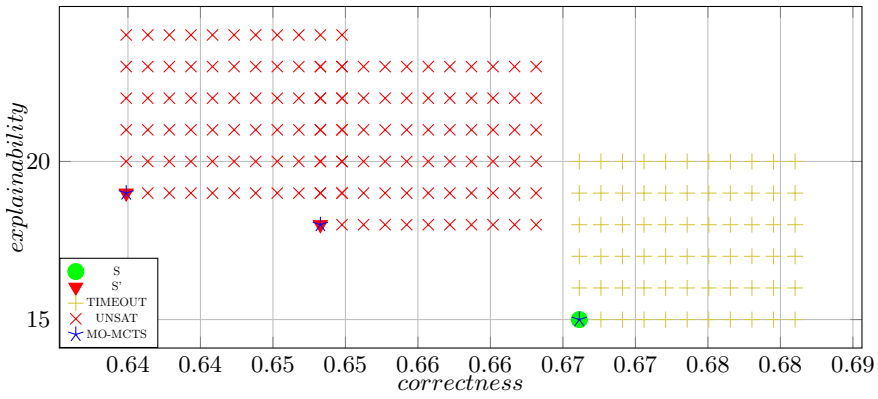

Fig. 19: national poll on healthy aging npha

Feature Names	Weights	Output Branches
f1	2	2
f2	2	2
f3	2	2
f4	2	2
f5	2	2

Table 13: List of feature names, weights and output branches

data1 This represents the benchmark data1. This benchmark uses a custom made black-box model. It restricts the space of decision trees to those with size at most 5. We present the feature names, weights and partition in Table 13.

Figure 20 plots the results.

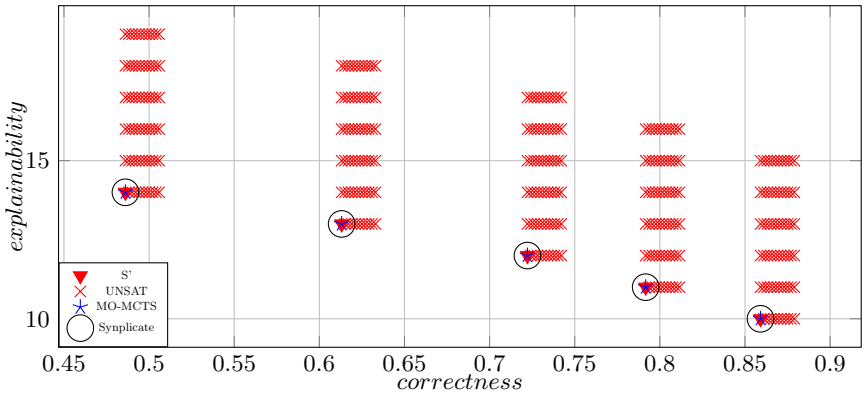

Fig. 20: data1

Feature Names	Weights	Output Branches
f1	2	2
f2	2	2
f3	2	2
f4	2	2
f5	2	2

Table 14: List of feature names, weights and output branches

data2 This represents the benchmark data2. This benchmark uses a custom made black-box model. It restricts the space of decision trees to those with size at most 5. We present the feature names, weights and partition in Table 14.

Figure 21 plots the results.

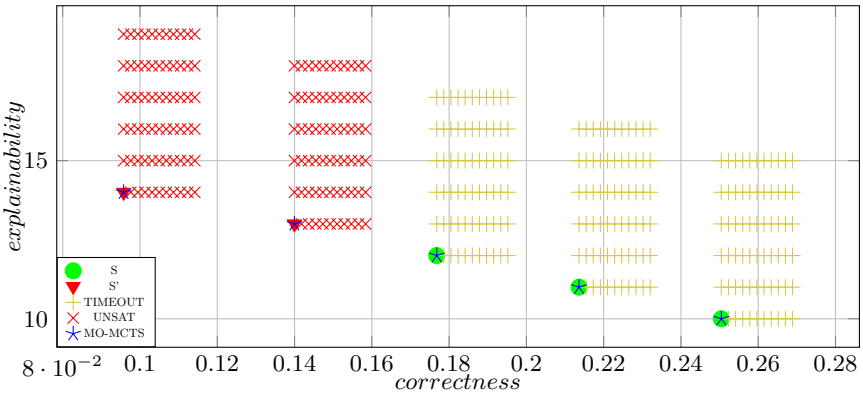

Fig. 21: data2

Feature Names	Weights	Output Branches
f1_2	3	3
f2_2	3	3
f3_2	3	3
f4_2	3	3

Table 15: List of feature names, weights and output branches

data218 This represents the benchmark data218. This benchmark uses a custom made black-box model. It restricts the space of decision trees to those with size at most 3. We present the feature names, weights and partition in Table 15.

Figure 22 plots the results.

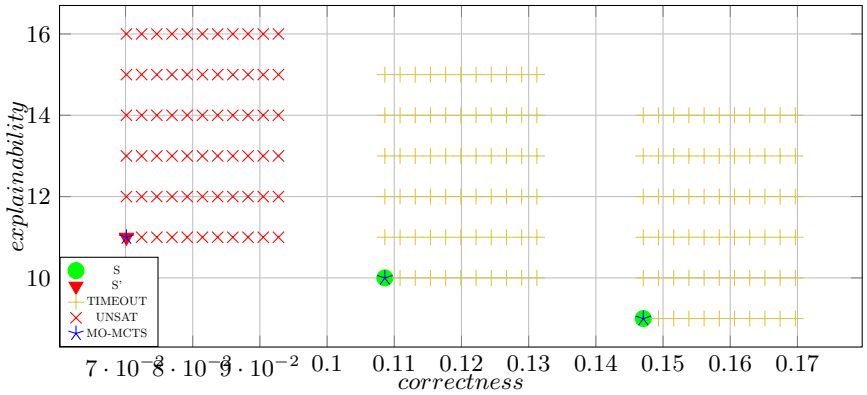

Fig. 22: data218

Feature Names	Weights	Output Branches
f0	2	5
f1	2	2
f2	2	6
f3	2	5
f4	2	4

Table 16: List of feature names, weights and output branches

random 1 This represents the benchmark random 1. This benchmark uses a custom made black-box model. It restricts the space of decision trees to those with size at most 5. We present the feature names, weights and partition in Table 16.

Figure 23 plots the results.

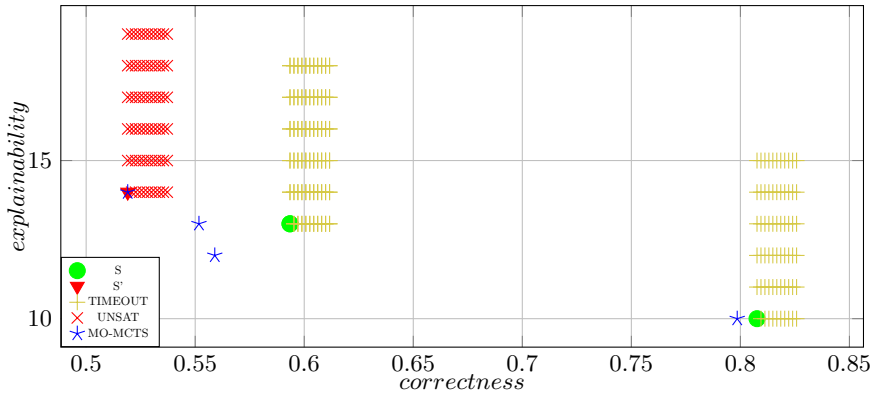

Fig. 23: random 1

Feature Names	Weights	Output Branches
f0	3	2
f1	3	4
f2	3	3
f3	3	2
f4	3	5

Table 17: List of feature names, weights and output branches

random 2 This represents the benchmark random 2. This benchmark uses a custom made black-box model. It restricts the space of decision trees to those with size at most 5. We present the feature names, weights and partition in Table 17.

Figure 24 plots the results.

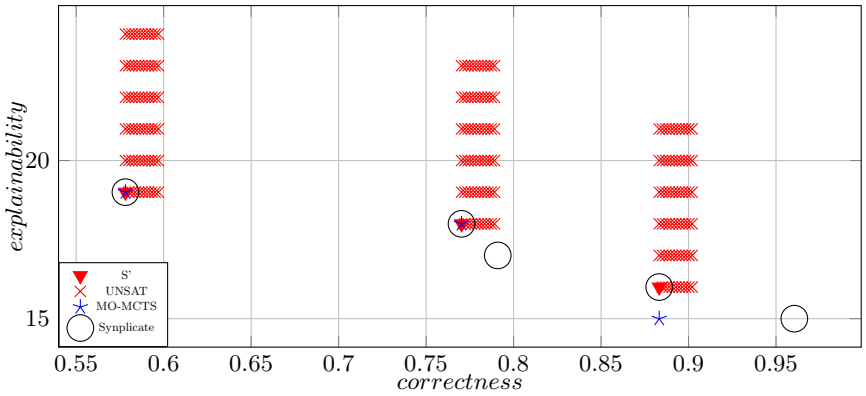

Fig. 24: random 2

Feature Names	Weights	Output Branches
f0	3	2
f1	3	2
f2	3	2

Table 18: List of feature names, weights and output branches

random 7 This represents the benchmark random 7. This benchmark uses a custom made black-box model. It restricts the space of decision trees to those with size at most 3. We present the feature names, weights and partition in Table 18.

Figure 25 plots the results.

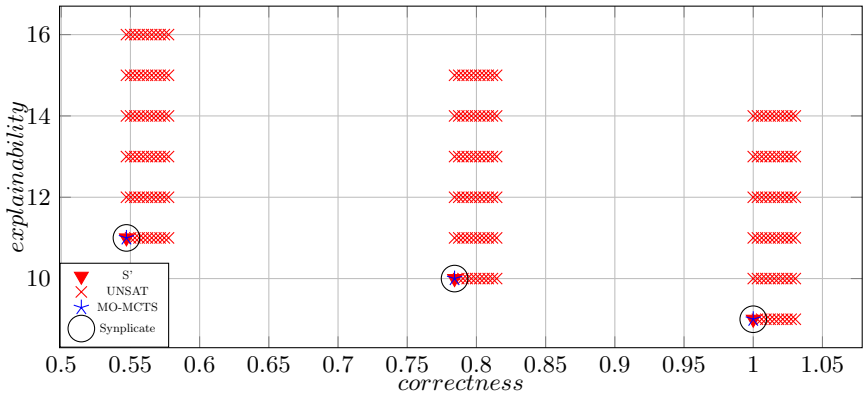

Fig. 25: random 7

Feature Names	Weights	Output Branches
f0	3	3
f1	3	5
f2	3	2
f3	3	3

Table 19: List of feature names, weights and output branches

random 9 This represents the benchmark random 9. This benchmark uses a custom made black-box model. It restricts the space of decision trees to those with size at most 4. We present the feature names, weights and partition in Table 19.

Figure 26 plots the results.

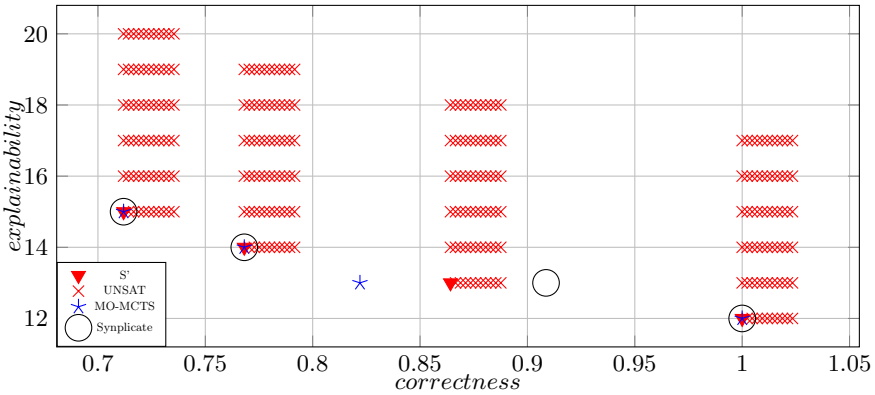

Fig. 26: random 9

Feature Names	Weights	Output Branches
f0	3	5
f1	3	4
f2	3	5
f3	3	3

Table 20: List of feature names, weights and output branches

random 10 This represents the benchmark random 10. This benchmark uses a custom made black-box model. It restricts the space of decision trees to those with size at most 5. We present the feature names, weights and partition in Table 20.

Figure 27 plots the results.

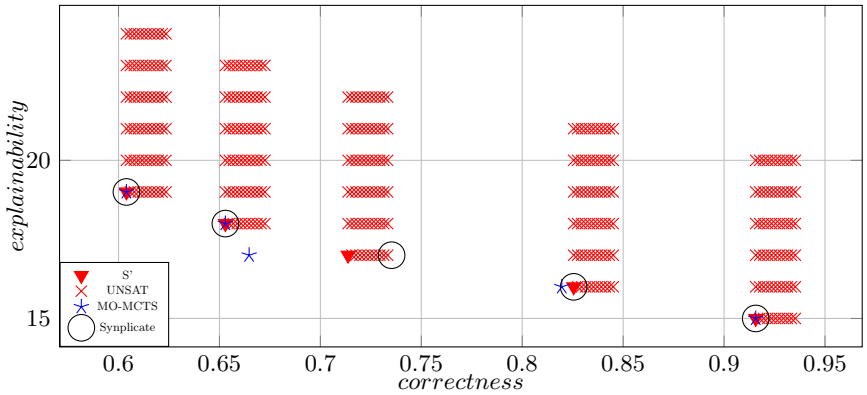

Fig. 27: random 10

C Extended Experiments 5 mins

We now present the results of running ALPO and Synplicate with a reduced overall timeout of 5 mins. For ALPO, this means we allocated 2.5 mins for the first phase (MO-MCTS), and 2.5 mins for the second phase. Our results show that ALPO gracefully degrades with less time being made available, but is still able to generate several LPO interpretations. However, Synplicate practically fails to generate anything (except one PO interpretation for Balance Scale) other than for Auto Taxi. This demonstrates the strength of ALPO as an anytime algorithm.

Feature Names	Weights	Output Branches
clouds_6	1	6
day_time_3	4	3
init_pos_4	3	4

Table 21: List of feature names, weights and output branches

AutoTaxi This represents the benchmark AutoTaxi used earlier. We restricts the space of decision trees to those with size at most 5. We present the feature names, weights and partition in Table 21.

Figure 28 plots the results.

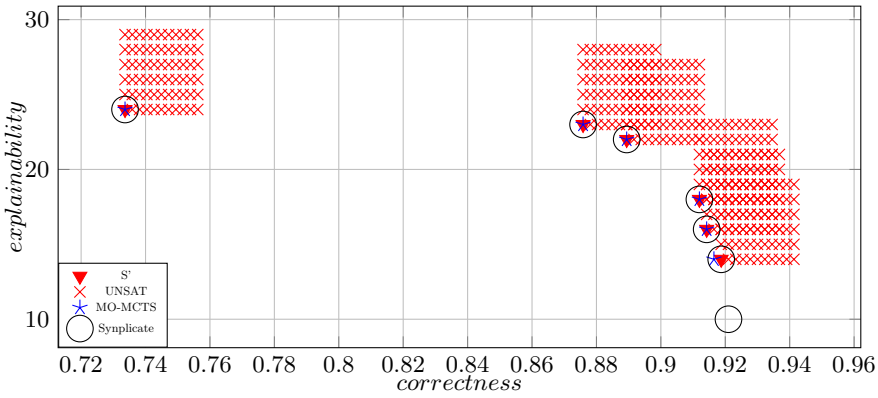

Fig. 28: AutoTaxi

Feature Names	Weights	Output Branches
left_distance	3	3
left_weight	3	3
right_distance	3	3
right_weight	3	3

Table 22: List of feature names, weights and output branches

balance scale This represents the benchmark balance scale. This benchmark uses a neural network trained on the dataset [32] from the UCI repository. It restricts the space of decision trees to those with size at most 5. We present the feature names, weights and partition in Table 22.

Figure 29 plots the results.

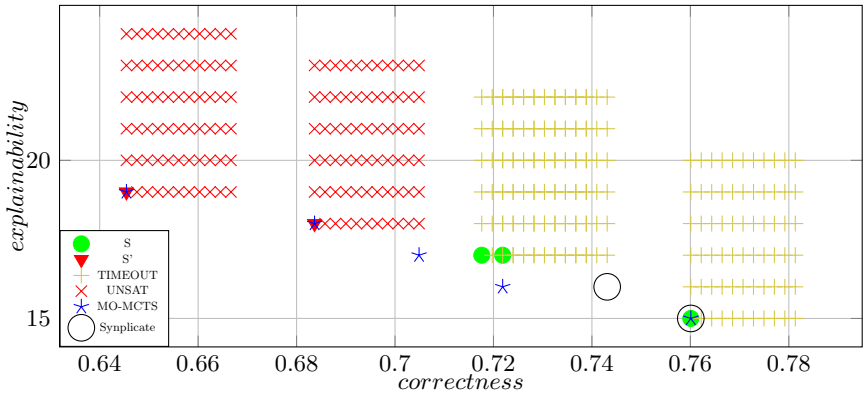

Fig. 29: balance scale

Feature Names	Weights	Output Branches
buying	3	4
doors	3	4
lug_boot	3	3
maint	3	4
persons	3	3
safety	3	3

Table 23: List of feature names, weights and output branches

car evaluation This represents the benchmark car evaluation. This benchmark uses a neural network trained on the dataset [8] from the UCI repository. It restricts the space of decision trees to those with size at most 5. We present the feature names, weights and partition in Table 23.

Figure 30 plots the results.

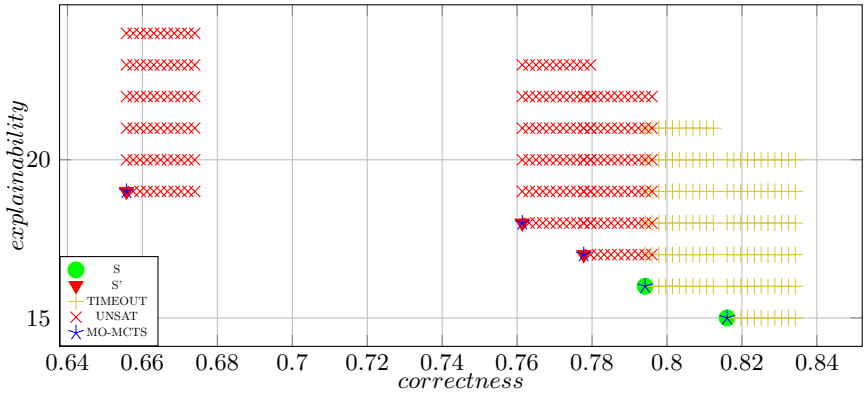

Fig. 30: car evaluation

Feature Names	Weights	Output Branches
alm	3	3
erl	3	3
gvh	3	3
mcg	3	3
mit	3	3
nuc	3	3
pox	3	3
vac	3	3

Table 24: List of feature names, weights and output branches

yeast This represents the benchmark yeast. This benchmark uses a neural network trained on the dataset [26] from the UCI repository. It restricts the space of decision trees to those with size at most 5. We present the feature names, weights and partition in Table 24.

Figure 31 plots the results.

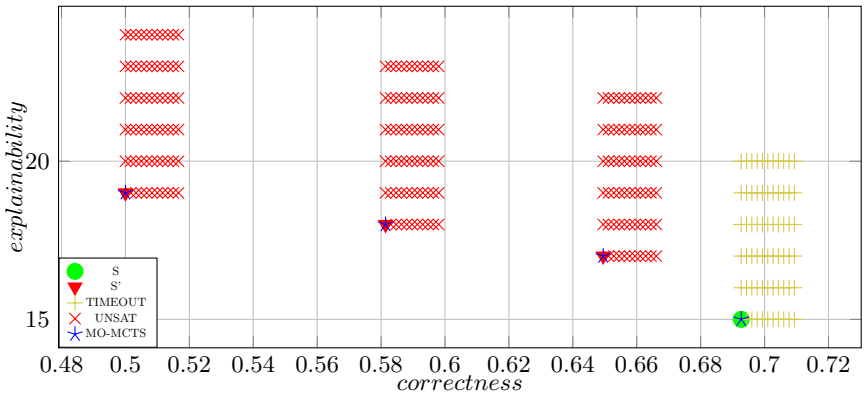

Fig. 31: yeast